

Factors influencing chlorophyll a concentrations in the Waikato River

Drivers of phytoplankton production in Lake Karapiro

Prepared for DairyNZ

January 2015



Authors/Contributors:

Max Gibbs, NIWA
Karl Safi, NIWA
Anathea Albert, NIWA
Ian Duggan, University of Waikato
Eddie Bowman, NIWA
David Burger, DairyNZ

For any information regarding this report please contact:

Max Gibbs
Water Quality Scientist
Freshwater Ecology
+64-7-856 1773
max.gibbs@niwa.co.nz

National Institute of Water & Atmospheric Research Ltd
PO Box 11115
Hamilton 3251

Phone +64 7 856 7026

NIWA Client Report No:	HAM2014-059
Report date:	January 2015
NIWA Project:	DNZ14204

Cover photo: Lake Karapiro reflections [Photo by Max Gibbs].

© All rights reserved. This publication may not be reproduced or copied in any form without the permission of the copyright owner(s). Such permission is only to be given in accordance with the terms of the client's contract with NIWA. This copyright extends to all forms of copying and any storage of material in any kind of information retrieval system.

Whilst NIWA has used all reasonable endeavours to ensure that the information contained in this document is accurate, NIWA does not give any express or implied warranty as to the completeness of the information contained herein, or that it will be suitable for any purpose(s) other than those specifically contemplated during the Project or agreed by NIWA and the Client.

Contents

- Executive summary 6**

- 1 Introduction 8**
 - 1.1 Present study 9

- 2 Methods 10**
 - 2.1 Site selection 10
 - 2.2 Physicochemical parameters 11
 - 2.3 Bioassays 13
 - 2.4 Nutrient bioassay 15
 - 2.5 Zooplankton grazing effects bioassay 16
 - 2.6 Sediment traps 16
 - 2.7 Current measurements 17

- 3 Results 18**
 - 3.1 River flows 18
 - 3.2 Temperature and dissolved oxygen 19
 - 3.3 Water quality 25
 - 3.4 Phytoplankton and Zooplankton 33
 - 3.5 PPR Bioassays 35
 - 3.6 Nutrient addition bioassay 38
 - 3.7 Zooplankton dilution experiment 39
 - 3.8 Acoustic Doppler Current Profiler (ADCP) 39

- 4 Discussion 46**
 - 4.1 Summary 47
 - 4.2 Conclusions 50

- 5 Acknowledgements 52**

- 6 References 53**

- Appendix A Phytoplankton 55**

- Appendix B Zooplankton 56**

- Appendix C Sediment traps 57**

Tables

Table 1:	Site locations, distance below Lake Arapuni and maximum and mean water depths.	10
Table 2:	Sample date, mean flow, incubation depths, dominant phytoplankton spp, and dominant zooplankton sp.	19
Table 3:	Nutrient data from the five monitoring sites and the upstream source water from Lake Arapuni on the four sampling occasions.	26
Table 4:	Mean current velocities (m/s) in the upper and lower water column at each site.	43

Figures

Figure 1:	Water quality at Waikato River sites during 1993-2012 for B) nitrate-N, D) Total P, and E) Chlorophyll a.	8
Figure 2:	Site map for Lake Karapiro and the Waikato River downstream of Lake Arapuni	11
Figure 3:	Richard Brancker Research model XR620F lake conductivity-temperature profiler	12
Figure 4:	PPR bottles assembled in a net bag attached to an incubation line ready for deployment.	15
Figure 5:	Dual collector sediment traps.	16
Figure 6:	Lake Karapiro discharge (upper) and water level (lower) December 2013 to May 2014.	18
Figure 7:	Temperature differences (ΔT) greater than 0.5 °C for more than 24 hours indicate thermal stratification.	19
Figure 8:	Time-series temperature data from the thermistor chain relative to flow through Lake Karapiro (right hand axis).	20
Figure 9:	Time-series dissolved oxygen (DO) data at three depths from the thermistor chain relative to flow through Lake Karapiro (right hand axis).	20
Figure 10:	Time series of bottom DO, thermal stratification (ΔT) and lake level in February 2014.	21
Figure 11:	Time-series temperature (upper) and dissolved oxygen (lower) data from the thermistor chain relative to flow through Lake Karapiro (right hand axis)	22
Figure 12:	Temperature and DO profiles at individual sites on the four incubation dates.	25
Figure 13:	Upper water column TN and TP concentrations on the four sampling occasions.	27
Figure 14:	Dissolved reactive phosphorus (DRP) concentrations in the upper 5 m and bottom water at each site on each occasion.	27
Figure 15:	Nitrate nitrogen ($\text{NO}_3\text{-N}$) concentrations in the upper 5 m and bottom water at each site on each occasion.	28
Figure 16:	Ammonium ($\text{NH}_4\text{-N}$) concentrations in the upper 5 m and bottom water at each site on each occasion.	28
Figure 17:	Chlorophyll a concentrations in the upper 5 m and bottom water at each site on each occasion.	29
Figure 18:	Depth profiles of temperature and chlorophyll at each site in December 2013.	30

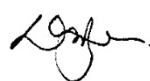
Figure 19:	Depth profiles of temperature and chlorophyll at each site in January 2014.	31
Figure 20:	Depth profiles of temperature and chlorophyll at each site in March 2014 .	32
Figure 21:	Depth profiles of temperature and chlorophyll at each site in May 2014.	33
Figure 22:	Changes in phytoplankton species composition and abundance between sites and between sampling dates.	34
Figure 23:	Zooplankton biomass at the five sites on each of the four sampling occasions.	35
Figure 24:	PPR results plotted as net carbon uptake rates in $\text{mg C m}^{-3} \text{ d}^{-1}$ for the five sites on each of the four sampling visits.	36
Figure 25:	Photosynthetically available radiation (PAR) light records for the four sampling visits.	37
Figure 26:	A set of underwater light profiles measured on 4 December 2013.	37
Figure 27:	Nutrient addition bioassay results showing the response to the addition of N, P and N+P as a proportional increase relative to the control.	38
Figure 28:	Nutrient addition bioassay results showing chlorophyll-a concentrations in the control (C) and N, P and N+P addition.	38
Figure 29:	Plots of growth relative to dilution in the zooplankton dilution incubations at site 2 and 5 in March 2014.	39
Figure 30:	Depth-Distance current velocity profile contours at site 2 .	40
Figure 31:	Depth-Distance current velocity profile contours at site 3.	40
Figure 32:	Depth-Distance current velocity profile contours at site 4 .	41
Figure 33:	Depth-Distance current velocity profile contours at the Buoy site.	41
Figure 34:	Depth-Distance current velocity profile contours at site 5.	42
Figure 35:	Depth-Distance current velocity profile contours near the dam.	42
Figure 36:	Longitudinal schematic diagrams of chlorophyll distribution (upper) and stylised flow paths (lower) in Lake Karapiro on 13 March 2014.	44
Figure 37:	Changes in chlorophyll mass relative to concentration at the 5 sites on each of 4 occasions.	47

Reviewed by



Graham McBride

Approved for release by



David Roper

Formatting checked by



Executive summary

Waikato Regional Council monitoring data from the Waikato River for the last 20 years show that there have been trends of decreasing chlorophyll *a* but increasing total nitrogen (TN) concentrations in the water. During this period, total phosphorus (TP) concentrations have remained relatively constant suggesting a knowledge gap or a lack of understanding of the factors that affect primary production in the Waikato River system. This report presents the findings of a series of four bioassay studies run in Lake Karapiro under different flow conditions from 5 locations along the lake to assess the effects of retention time and thermal stratification in the hydro lakes on chlorophyll *a* concentrations in the Waikato River.

Phytoplankton dynamics

Measurements of primary production and respiration (PPR) as net carbon uptake rates in the upper 5 m of the water column show that seasonal growth of phytoplankton in Lake Karapiro mostly occurs in January to March, when water discharges are lowest and residence time is highest.

Transect data on each sampling occasion showed that chlorophyll *a* concentrations generally increased with distance from Lake Arapuni, with highest concentrations in the upper mixed water column, coinciding with higher water temperatures, thermal stratification, and increased residence times associated with lower flow rates through Karapiro dam. Profiling data identified that the presence and depth of the upper mixed layer was regulated by draw-induced stratification associated with the high level outflow from the power station.

Stratification appeared to induce higher growth rates by confining the phytoplankton in the water column above the critical depth¹. Channel morphometry had a strong influence on the critical mixing depth in the mid-reaches of the lake (Site 3), where deeper mixing reduced phytoplankton productivity during periods of high and medium flow.

Nutrient limitation bioassays in March indicated possible N limitation of phytoplankton growth at all sites and possible P stimulation at sites 1 and 3 as well. Addition of both N and P stimulated additional growth at all sites (i.e., co-limitation) implying that there was nutrient depletion in the upper water column at that time. Nutrient availability is likely to exert a greater influence on phytoplankton biomass than zooplankton grazing at the downstream sites, when surface chlorophyll *a* concentrations are high. Zooplankton grazing may become important when Cladocera are dominant and may favour the dominance of large diatom species, which would be difficult to ingest.

Lake nutrient cycling

Increasing concentrations of dissolved reactive phosphorus (DRP) and ammonium (NH₄-N) in the bottom waters of the lake with increasing distance downstream from Lake Arapuni suggest that in-lake processes do contribute to the internal nutrient cycling. Differences between surface and bottom water nutrient concentrations showed an apparent stoichiometric reduction in DRP and nitrate (NO₃-N) concentrations relative to an increase in chlorophyll *a* concentrations in the upper water column. This implies that these differences were mostly due to phytoplankton uptake and growth in the upper water column rather than nutrient increases in the lower water column.

¹ Critical depth in well mixed water column is the theoretical depth at which phytoplankton growth in the upper well lit water column is matched by the losses of biomass in lower dark water column.

Factors influencing phytoplankton growth

The key factors influencing phytoplankton growth in Lake Karapiro in summer have been identified as temperature, light, residence time, nutrient availability and draw-induced stratification — normally controlled by temperature (thermal stratification) but stratification can also be regulated by depth of draw and flow through the power station. Stratification confines phytoplankton in the well-lit upper water column above critical depth. Maximum algal production is supported by nutrient availability, provided the phytoplankton have sufficient residence time to utilise those nutrients. There will be a direct relationship between growth and residence time such that as residence time decreases, growth will decrease.

Nutrient availability will be affected by in-lake cycling and the isolation between bottom and surface water caused by stratification. It will also be supplemented by groundwater and stream inflows. However, nutrients from these inputs are likely to be largely removed by riparian and littoral vegetation, including aquatic macrophytes and the epiphytes growing on the macrophyte leaves.

In Lake Karapiro the growth and decay of the macrophyte hornwort (*Ceratophyllum demersum*) is likely to have an impact on phytoplankton nutrient availability. While the magnitude of this impact is currently unclear, the presence of extensive macrophyte beds in the lake, as well as frequent detachment and transport of plant mats further downstream due to changing flow patterns, means their effect is likely to be significant.

1 Introduction

The National Policy Statement (NPS) for Freshwater Management provides a national framework that directs how councils are to go about setting objectives, policies and rules about fresh water in their regional plans. Councils must do this by establishing freshwater management units across their regions and identifying the values that communities hold for the water in those areas. To achieve this, councils are required to gather water quality and quantity information on the water bodies to assess their current state and decide the water quality objective or goal for each value the community has chosen. Concentrations of chlorophyll *a*, total nitrogen (TN) and total phosphorus (TP) are national attributes in the NPS for lakes and are therefore the indicators of the current state of the water quality and water quality changes over time, that need to be managed.

Information presented at the Waikato Economic Impact Joint Venture, Phase 2 – Water Quality meeting on 12 September 2013 raised concerns about a knowledge gap that could affect economic modelling related to river water quality. Long-term monitoring data from 9 locations down the main stem of the Waikato River (Vant 2013) show variability between sites for the phytoplankton biomass (indicated by chlorophyll *a* concentrations) and the concentrations of TN and TP in the water. These data show that there have been trends of decreasing chlorophyll *a* ($-2.1\% \text{ y}^{-1}$) but increasing TN ($+1.5\% \text{ y}^{-1}$) concentrations, especially in the last 10 years. These data also show that TP concentrations have remained relatively constant over the 20 year data period, but may now show a weak trend of decrease (Figure 1).

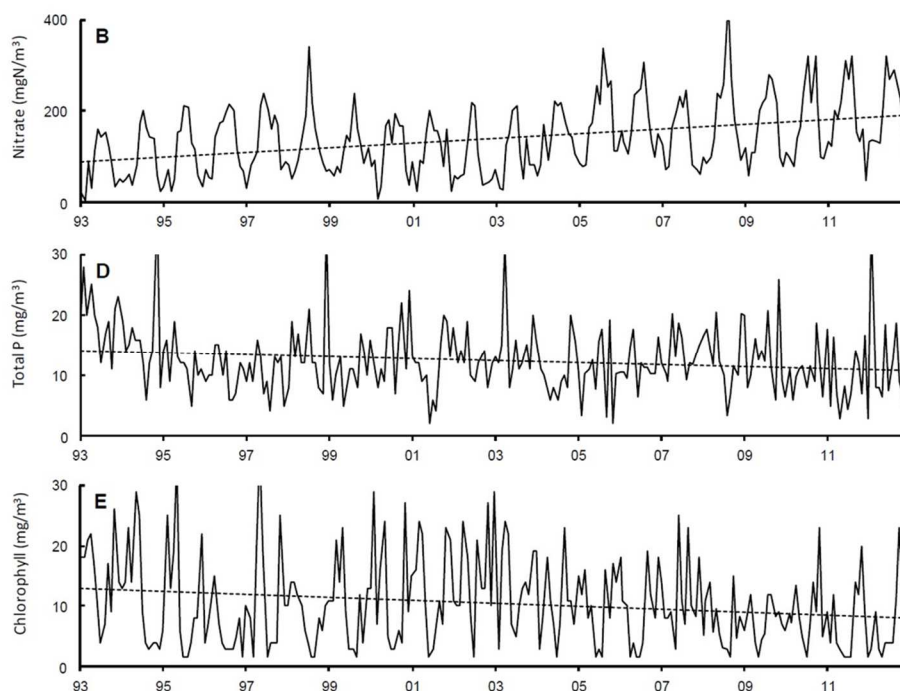


Figure 1: Water quality at Waikato River sites during 1993-2012 for B) nitrate-N, D) Total P, and E) Chlorophyll *a*. (Data extracted from Vant 2013, Figure 2).

The expectation would be for phytoplankton biomass to increase in response to the increase in TN, which is mainly in the form of biologically available nitrate-nitrogen ($\text{NO}_3 \text{ N}$). This is because the Waikato River system has historically been thought to be N not P limited and water quality models for the Waikato River have been parameterised to reflect this (Rutherford et al. 2001). That

chlorophyll *a* concentrations are actually decreasing, points to a knowledge gap or lack of understanding of the factors that influence primary production in the Waikato River system.

Nutrient limitation, phytoplankton species and zooplankton grazing in the Waikato River excluding the hydro lakes are the subjects of a separate study Waikato Regional Council.

1.1 Present study

This report presents the findings of a study using Lake Karapiro as an example to understand what influences phytoplankton growth, and thus chlorophyll *a* concentrations in the Waikato River. The study is part of the Healthy Rivers Plan for Change (Waikato Regional Council 2014) process focussing on a better understanding of algal dynamics in the hydro lakes, which is critical to protecting and restoring the health and wellbeing of the Waikato River. This information is intended to contribute to a better understanding of the causes of temporal trends in nitrogen and chlorophyll *a* in the main stem of the Waikato River and to inform river models.

The information in this report comprises the results of three discrete studies from five locations in Lake Karapiro spaced upstream from the dam to Finlay Road Camp (Figure 2), at high, medium, and low flow conditions and a fourth study when lake Karapiro was thermally stratified. On each study occasion, the measurements included:

- Primary production and respiration (PPR) to assess phytoplankton growth. This assay used 24-hour, carbon-14 (¹⁴C) uptake techniques to measure actual growth expressed as mg C m⁻³ d⁻¹.
- Depth related temperature, dissolved oxygen, light and chlorophyll fluorescence profiles.
- Water clarity (Secchi depth).
- Water quality in the upper and lower water column.
- Zooplankton and phytoplankton enumeration in the upper water column.
- Sedimentation.
- Time-series temperature and dissolved oxygen (DO).
- Flow data.
- Ambient light.

Time series temperature and dissolved oxygen was continuous for the duration of the study. On one occasion, current flow velocities were measured at each site downstream of Horahora Bridge.

The data are presented graphically or in tables with all numerical data provided in the appendices.

2 Methods

2.1 Site selection

A preliminary reconnaissance survey of Lake Karapiro on 27 November 2013 was used to select five monitoring sites along the length of the lake (Table 1, Figure 2) and to establish transit times between sites for the planning of incubation experiments. This visit was also used to establish a suitable location for, and deployment of, a thermistor chain with dissolved oxygen (DO) sensors (Figure 2).

It was decided that, because of the transit time to collect water for incubations, all incubations would be undertaken at the buoy site rather than at the collection site. That way, all samples would be incubated for the same length of time, at the same temperature and under the same light conditions.

The buoy site was located in the middle of the lake in 27 m depth of water about 100m upstream of a weed boom chain across the lake. This position was out of the rowing lanes, which were on both sides of the lake and upstream of any regatta courses (Figure 2).

Morphometric data (Table 1) were taken from depth profiles at each site (max Depth) and the current profiler transects in March 2014 (mean Depth). Mean depths and open channel widths were estimated as the effective open water channel between weed beds and submerged shallows at each site. (See section 3.8 for more information).

Table 1: Site locations, distance below Lake Arapuni and maximum and mean water depths. Mean depths and site widths are best estimates from the current profiling data.

Site Code	Description	NZTM coordinates		Distance from L. Arapuni (km)	Max Depth (m)	Mean Depth (m)	Est. Width (m)
		E	N				
Arapuni	River from Road bridge	1832030	5783380	0			
Site 1	Pokaiwahenua confluence	1833480	5792150	8.7	11	7	140
Site 2	Horahora Bridge (downstream)	1833410	5796150	12.8	22	11	120
Site 3	Cliffs	1828780	5796610	18.0	30	17	120
Site 4	Pylons	1826030	5797200	20.7	28	13	180
Site 5	Rowing club	1823770	5798830	23.8	29	12	320
Additional sites							
Dam	Upstream of Karapiro dam boom	1823410	5799400	24.5	35	12	
Buoy	Upstream of Weed boom	1824600	5797600	21.6	27	12	250

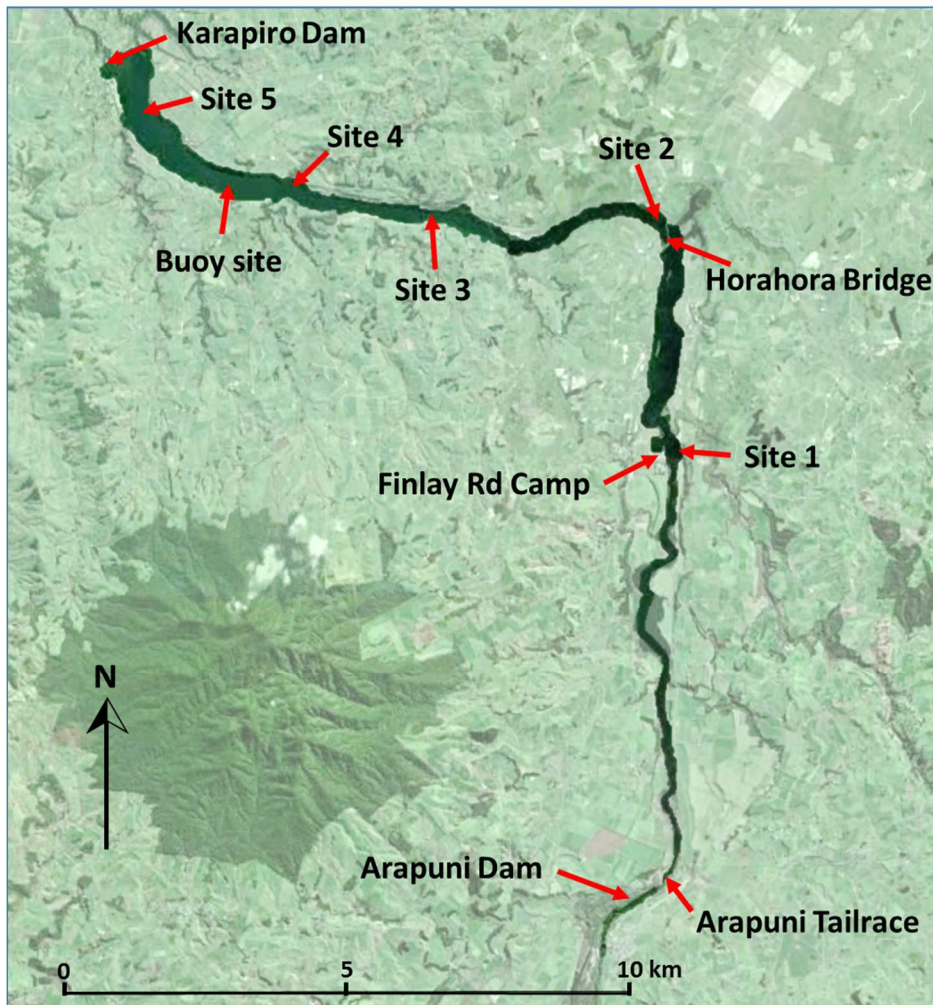


Figure 2: Site map for Lake Karapiro and the Waikato River downstream of Lake Arapuni showing the sampling sites, the location of the thermistor chain buoy, which was also the incubation site, and other key landmarks. Site 1 is at the confluence of the Pokaiwhenua Stream with the Waikato River.

2.2 Physicochemical parameters

2.2.1 Temperature

A thermistor chain was constructed by attaching Onset HOBO Water Temp Pro v2 loggers or Onset U26 dissolved oxygen loggers to a non-stretch, braided 6-mm cord at 1-m intervals from 1 m below a surface buoy to a depth of 26 m below the surface in 27 m water depth. The DO loggers were installed at 2 m, 20 m and 26 m, to check for bottom water anoxia.

The thermistor chain was deployed three times. The first time, on 27 November 2013, covered the period before the 4 December 2013 sampling and up to 22 December 2013. At that time the weed boom was removed and someone from Rowing New Zealand retrieved the thermistor chain and put it in a storage shed. It was not located until mid-January 2014. The second deployment was from 23 January to 29 April 2014, which covered the samplings on 30 January and 19 March 2014 as well as the ADCP current survey on 13 March 2014. The thermistor chain was removed because of the risk it would be lost with the masses of drifting weed as the lake discharge increased after the extended period of low flow. The third deployment was for the period of the sampling on 7 May 2014.

2.2.2 Water column structure

During the preliminary survey and each subsequent sampling visit, temperature, DO, chlorophyll fluorescence and light profiles through the full depth of the water column were measured at each sampling location along the central axis of the lake with a Richard Brancker Research model XR620F lake profiler (Figure 3). Water clarity was assessed by Secchi depth using a 20-cm black and white quartered disc on a tape measure at each sampling site. The Secchi depth value was used to set the incubation depths for the *in situ* PPR assays namely upper at half the Secchi depth, middle at full Secchi depth and lower at 2.5 times the Secchi depth.

Ambient light levels were recorded using a 2π Licor photosynthetically available radiance (PAR) sensor on a roof in Cambridge. The recording covered the full 24 hour incubation period.

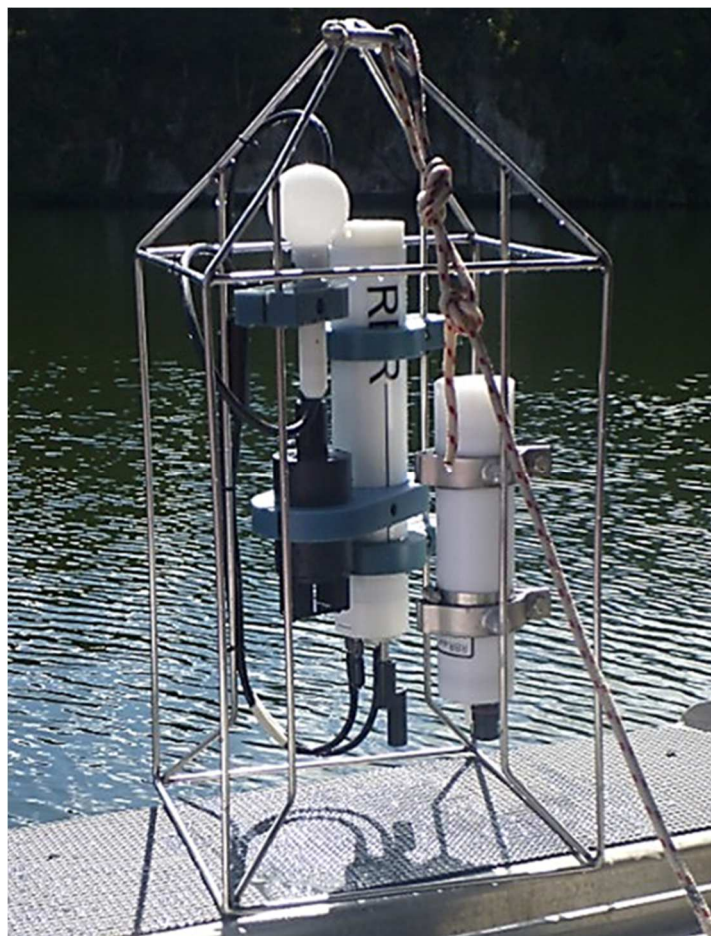


Figure 3: Richard Brancker Research model XR620F lake conductivity-temperature profiler fitted with a Licor biospherical 4π PAR sensor, a Seapoint chlorophyll fluorescence sensor and a RBR Duo dissolved oxygen-temperature sensor.

2.2.3 Water Sampling

On the first sampling trip, upstream water was collected by boat from the turbulent river several km upstream of Site 1 as being representative of the water quality entering Lake Karapiro. However, because this increased the transit time on the water by more than an hour, on subsequent sampling trips, the upstream water sample was collected from the road bridge below the Arapuni Dam (Arapuni Tailrace, Figure 2), using a weighted 10-litre bucket on a rope. This water was returned to the laboratory for processing while the lake samples were still being collected for the incubations.

Water samples were collected at each of the five monitoring sites as depth-integrated samples from the upper water column using a 5-m long by 20-mm diameter integrated tube sampler lowered vertically through the upper water column, keeping the water level inside the tube at the same level as the water level outside the tube. To obtain sufficient water for the incubations and other measurements being made, multiple collections were made and were combined in a 20 L plastic bucket. This water was mixed by stirring immediately before separate aliquots were taken in 5-L bottles for the PPR incubations and nutrient analyses. A bottom water sample was collected for nutrient analyses using a horizontal van Dorne-type water sampling bottle.

For the nutrient addition bioassay, water was sieved through a separate, specially cleaned funnel fitted with a 40 µm mesh to exclude the large zooplankton fraction.

2.2.4 Phytoplankton

Raw water was assessed for phytoplankton species composition by cell counts per unit volume and biomass was expressed as biovolume. Data are in Appendix A.

2.2.5 Zooplankton

For zooplankton enumeration and biomass, 40 L of water was passed through a 40 µm mesh zooplankton net and the zooplankton collected were preserved in 50% ethyl alcohol/water mixture, on site. Zooplankton species composition was determined at the UoW on the preserved sample. Zooplankton subsamples were enumerated in the laboratory at ~30x magnification under a stereo-dissecting microscope in aliquots until at least 300 individuals were encountered. Zooplankton biomass was estimated from the samples using length-weight relationships for crustaceans, and from tabulated median values, supplied by Lauridsen et al. (2005), for all other taxa. Where possible, at least 10 randomly encountered individuals of each crustacean species were measured. Data are in Appendix B.

2.3 Bioassays

2.3.1 ¹⁴C *In-situ* Primary Productivity (PPR) Incubations

Phytoplankton growth rate was estimated using net Primary Productivity (PPR) incubations following the method originally proposed by Steeman-Nielsen (1952). This PPR method measures actual carbon uptake rates rather than inferring productivity from photosynthetic oxygen production minus dark respiration. It used light and dark bottle incubations with the dark bottle results subtracted from the light bottle results to eliminate the effect of dark uptake and provide net primary production estimates.

Water samples collected by 0-5 m integrated sample tube from each site for PPR assays were kept in the dark at ambient temperatures in closed chilli bins, and were set up in the darkened cabin on the boat at the buoy site.

Three primary production incubation depths were used. The first was either 0.5 or 1 m below the surface depending on ambient light conditions (cloudy day vs sunny, respectively). The second was at the measured Secchi depth (~2.5m on most occasions) and the third at two and a half times the Secchi depth (~6-7m). These were equivalent to light levels of approximately 50%, 5% and 1% of surface irradiance.

For each depth incubation, triplicate 156 mL clear PET² bottles and triplicate dark PET bottles (controls) were rinsed with incubation water before being filled in low light conditions to avoid light shock.

Working stock ampules containing a ¹⁴C solution diluted with sodium bicarbonate of 47.7 µCi ml⁻¹ were opened and mixed together immediately before spiking all incubation bottles with 200 µl of working solution. This spike was also added to a PET bottle containing 100 ml of distilled water with NaSO₄ solution at concentration of 30 g l⁻¹, as a control.

Once all samples were spiked one depth from one site was randomly selected and 200 µl samples were removed and added to vials containing 250 µl of Ethanolamine. These were used to confirm stock solutions ¹⁴C concentrations. Similarly, 5 samples were taken from the 100 ml NaSO₄ solution and added to vials containing 250 µl of Ethanolamine again to confirm stock solutions ¹⁴C concentrations.

Bottles were grouped by site and depth and deployed at the buoy site on separate incubation lines. The bottles were taped together with clear sticky tape and supported in a mesh bag, which was cable-tied to the incubation line (Figure 4). The time of deployment was recorded and after ~24 hours samples were collected and returned to the Hamilton site for filtration.

A sample volume of 25-50 ml was filtered through a 0.2 µm polycarbonate filter. The filters were sucked dry and placed directly into 20 ml scintillation vials. The scintillation vials were acidified with 0.3 ml of 0.5 N hydrochloric acid (HCl) and placed under a fume hood overnight. Scintillation cocktail (5ml) was added and the samples were counted on a Perkin Elmer Tri-Carb 2910 TR liquid scintillation analyser within five days.

At each sampling site, water samples were collected in 60 ml screw-cap glass vials and preserved 2 drops of 0.5% mercuric chloride (HgCl₂) before sealing. These samples were analysed for dissolved inorganic carbon (DIC) on a Shimadzu TOC-VCSH total organic carbon analyser and the results were used to correct the PPR counts.

On the last sampling, the flow through Lake Karapiro had increased after several weeks of very low flows, which had allowed substantial growth of aquatic macrophytes (hornwort) along the sides of the lake. The increased flow dislodged masses of the hornwort, some of which caught on the PPR lines and compromised those incubations. The site 2 incubation was lost and recovered several days later.

² PET = polyethylene terephthalate is an optically clear and gas impervious plastic used for making beverage bottles. Bottles made from this material are typically referred to as PET bottles



Figure 4: PPR bottles assembled in a net bag attached to an incubation line ready for deployment. The dark control bottles were painted black and covered with black tape.

2.4 Nutrient bioassay

On the March 2014 sampling visit, nutrient addition bioassays were done following the method and protocols used by White and Payne (1977) on Lake Taupo. These were a 24 hour, in-situ growth assay on water that had been passed through a 40 μm sieve / plankton net (i.e., without large zooplankton). Nutrient additions of +P, +N and +N+P were compared with control water (no addition) to estimate the nutrient status of the phytoplankton in the water at each site at the time of sampling.

The 40 μm sieved water from each site was mixed and divided into 4 parts:

1. an addition of sodium nitrate to a final concentration of plus 140 mg m^{-3} as nitrate-N ($\text{NO}_3\text{-N}$) above background
2. an addition of potassium dihydrogen phosphate to a final concentration of plus 10 mg m^{-3} as dissolved reactive phosphorus (DRP) above background
3. additions of both N and P to final concentrations of plus 140 mg m^{-3} $\text{NO}_3\text{-N}$ and plus 10 mg m^{-3} DRP above background, and
4. no nutrient additions, to be used as the control.

The bioassay was set up using 2-litre, clear, Nalgene bottles attached to an incubation line and suspended 1 m below the surface at the buoy site. On retrieval, the bottles were mixed and three replicate 100 ml aliquots were filtered onto 2.5 cm diameter Whatman GF/C glass fibre filters. The filters were stored frozen in individual 'Secol' brand polycarbonate envelopes pending analysis for chlorophyll a .

Phytoplankton response to the nutrient additions was assessed as the proportional increase in chlorophyll a concentrations in the treatments relative to the control at the end of the incubation period.

2.5 Zooplankton grazing effects bioassay

On the March sampling visit, a zooplankton grazing effects bioassay was done as a 24 hour incubation based on the sequential dilution method of Gallegos et al. (1996) and others (e.g., Yu et al. 2010). The technique assumes that zooplankton filter feed on phytoplankton at a constant rate and that, as the sample is diluted, a point will be reached where the filtering efficiency of the zooplankton will be so reduced that phytoplankton growth will be unaffected.

The bioassay was conducted on raw water from sites 2 and 5 only. The sequential dilutions were made with filtered (Whatman GF/C glass fibre filter) water from the same site. This means the dilution water has the same chemical characteristics as the raw water but without zooplankton or phytoplankton. The bioassay was set up using 400 ml wide-mouth, clear, PET jars on an incubation table in a controlled temperature room at 18°C. Lighting consisted of a bank of 12 daylight fluorescent lights 0.5 m above the jars. The lights cycled on and off by timer for a 16 hour light and 8 hour dark cycle. Light levels were $\sim 170 \mu\text{Mol m}^{-2} \text{s}^{-1}$, which is equivalent to 20% of the average natural daily ambient photosynthetically available radiation (PAR).

Treatments consisted of diluting duplicate raw water with dilution factors of 1 (raw water control), 0.6, 0.4, 0.2, 0.1 and 0.05. Chlorophyll *a* concentration was measured in the initial water and then in all jars at the end of the 24 hour incubation period. Zooplankton grazing effects were assessed from the slope of each chlorophyll *a* concentration regression line, after correction for dilution at the end of the incubation period.

2.6 Sediment traps

On the first sampling visit, a dual collector sediment trap (Figure 5) was deployed at each of the selected sampling locations to be retrieved after five days. Unfortunately, the traps were overwhelmed by drifting weed and all were lost. On the second sampling visit another set of traps were deployed but three were lost due to weed drift. On the third sampling visit, traps were set at sites 4 and buoy, and a lost trap was recovered from site 3. On the fourth sampling visit, the three sediment traps were deployed at the buoy site in a vertical array at depths of 10 m, 20 m and 25 m below the surface to assess sediment resuspension.



Figure 5: Dual collector sediment traps. Upper cone opening is 150 mm diameter covered with a 10-mm square grid plate. The sediment is collected in 60 ml screw-cap jars.

2.7 Current measurements

In March 2014, under stratified and low flows conditions, in-lake currents were measured at sites 2, 3, 4 and 5, and across the lake near the dam using a boat mounted acoustic Doppler current profiler (ADCP) in bottom tracking mode. These data were used to assess the difference in flow patterns in the upper and lower water column.

Current flow through the lake was provided by Mighty River Power as discharge data from Lake Karapiro. The graphical presentation of this data was also recorded as a screen-grab from the Mighty River Power web site at

www.mightyriver.co.nz/Our-Business/Generation/Lake-Levels.aspx

showing the changes in flow for the previous 7 days.

3 Results

3.1 River flows

Mean flow over the duration of the experiments (Dec. 2013 to May 2014) was $184 \text{ m}^3/\text{s}$. Flow conditions on the individual sampling days were $306 \text{ m}^3/\text{s}$ (4 Dec. 2013), $206 \text{ m}^3/\text{s}$ (30 Jan. 2014), $156 \text{ m}^3/\text{s}$ (19 Mar. 2014) and $171 \text{ m}^3/\text{s}$ (7 May 2014), $158 \text{ m}^3/\text{s}$ (14 Mar. 2014) during the current measurements (Figure 6).

The flow classifications allocated to each experiment were based on the mean discharge from Lake Karapiro over the seven days before the PPR incubations (Table 2). Minimum flow through the lake was $144 \text{ m}^3 \text{ s}^{-1}$ during the extended low flow period from early March through early May 2014.

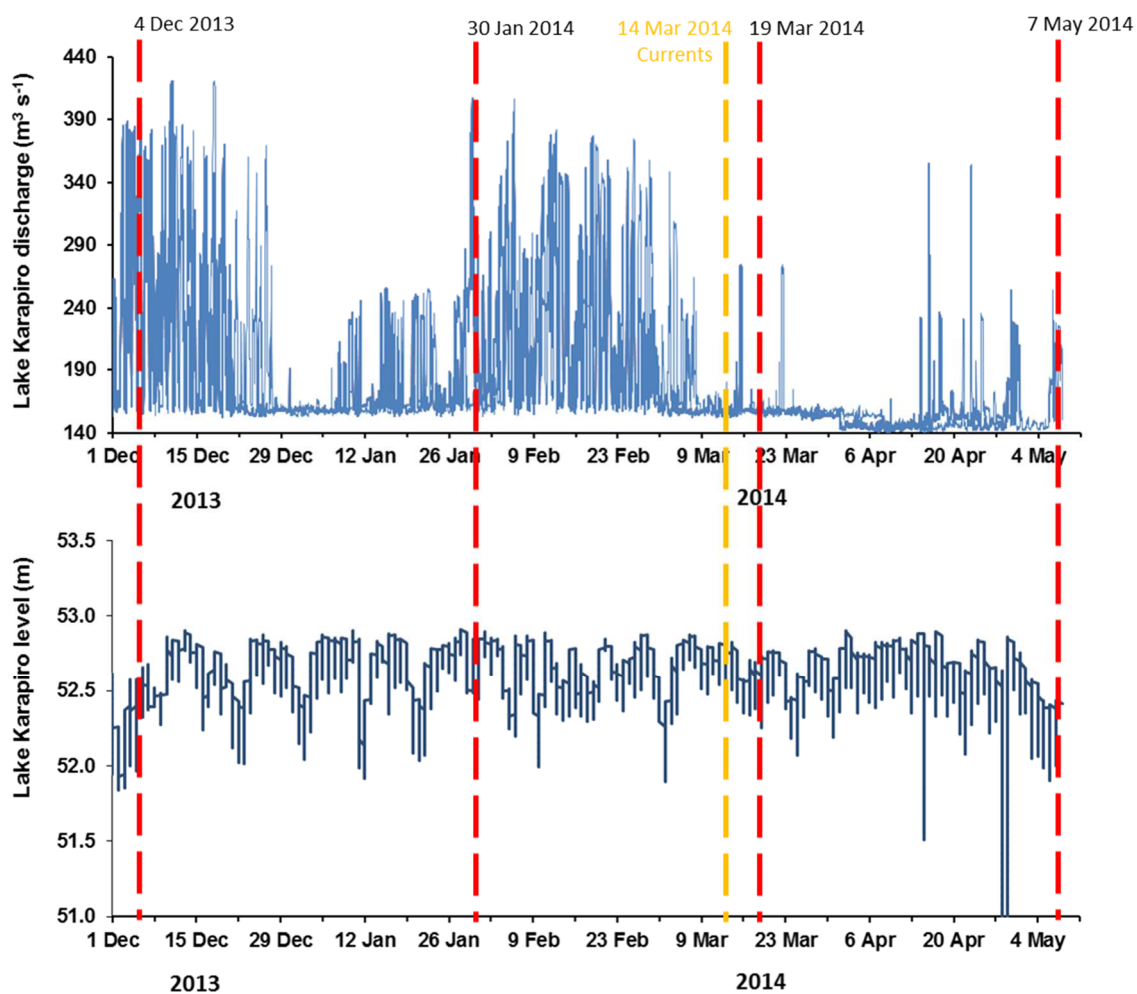


Figure 6: Lake Karapiro discharge (upper) and water level (lower) December 2013 to May 2014. Vertical broken lines are the sampling dates. Red lines are the incubation experiments, the orange line is the current measurement day. Data provided by Mighty River Power.

Table 2: Sample date, mean flow, incubation depths, dominant phytoplankton spp, and dominant zooplankton sp.

Sample Date	Mean flow (7 days before) (m ³ s ⁻¹)	Classification (by Flow)	Incubation depths			Dominant Phytoplankton	Dominant Zooplankton
			Upper (m)	Middle (m)	Lower (m)		
4-Dec-13	240	High	0.5	2.6	5.5	Diatoms <i>Fragilaria crotonesis</i>	Cladocerans <i>Bosmina meridionalis</i> <i>Daphnia galeata</i>
30-Jan-14	196	Medium	1.0	2.4	6.0	Diatoms <i>Fragilaria crotonesis</i>	Rotofers <i>Polyarthra dolichoptera</i>
19-Mar-14	163	Low (stratified)	1.0	2.4	6.0	Diatoms <i>Attheya sp</i>	Rotofers <i>Polyarthra dolichoptera</i>
7-May-14	168	Low (Mixed)	0.5	2.4	6.0	Diatoms <i>Aulacoseira sp</i>	Rotofers <i>Polyarthra dolichoptera</i>

3.2 Temperature and dissolved oxygen

The results of the thermistor chain located at Site 5 indicate that stratification occurred periodically over the summer period (Figure 7) and was influenced by flow rate through the Karapiro dam, inflow temperature and climatic conditions. Thermal stratification is occurring where the temperature difference between surface and bottom water is greater than 0.5 °C for more than 24 hours. Shorter duration temperature differences in the order of less than a day are due to surface warming. The “weed effect” was caused by drifting weed lifting the thermistor chain out of the water (Figure 7).

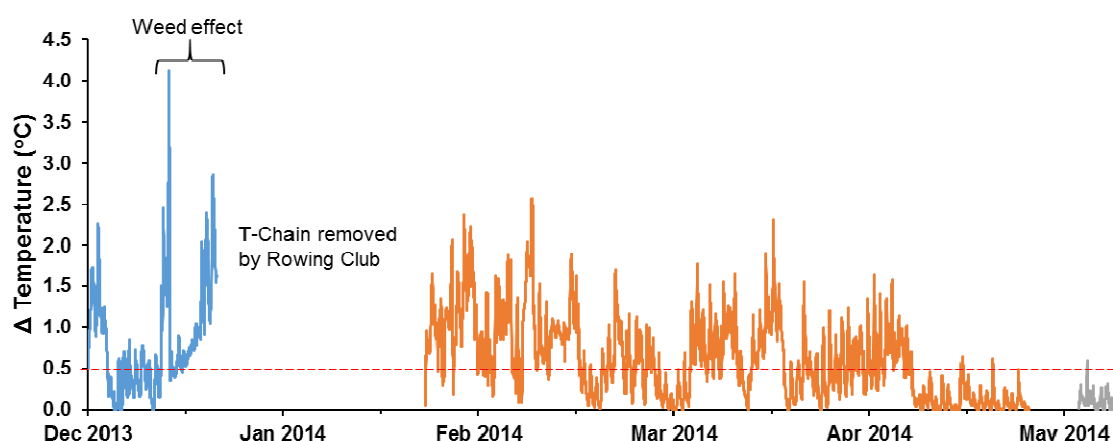


Figure 7: Temperature differences (ΔT) greater than 0.5 °C for more than 24 hours indicate thermal stratification. Daily surface water warming accounts for short duration temperature differences. Broken red line indicates a difference of 0.5 °C. The weed effect drew the thermistor chain out of the water.

Thermistor chain temperature data from the first deployment (Figure 8) show that the lake was thermally stratified at the end of November 2013. However, stratification at that time was due to cold water from Lake Arapuni moving through Lake Karapiro as an underflowing density current. This is seen as the bottom 5 m being about 1.5 °C colder in November than after 5 December. Conventional stable thermal stratification, where solar radiation warms the surface water relative to the deeper water, began around 16 December although there was evidence of daily surface warming through the whole record. The development of stable stratification coincided with a reduction in flow (Figure 8). The anomalous surface temperature spike from 12 to 14 December (Figure 8) was caused by drifting weed masses lifting the top of the thermistor chain out of the water. When the weed rolled away, the thermistor chain returned to its original position.

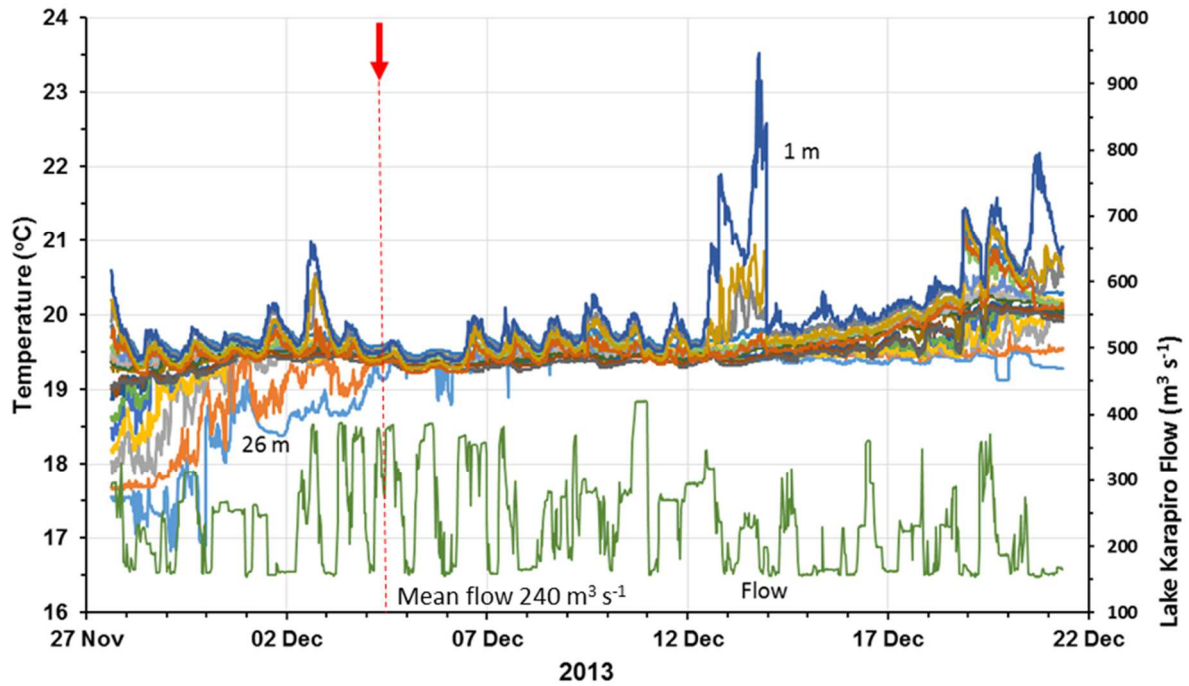


Figure 8: Time-series temperature data from the thermistor chain relative to flow through Lake Karapiro (right hand axis). Red arrow marks the first sampling visit (4 December 2013). Line colours encompass temperature sensors across 26 depths. Where the lines are all close together, the water column is well mixed. Where some of the lines are lower or higher than most of the lines, the water column is thermally stratified, either by cold bottom water or solar heating of surface water (cf. thermal stratification graph, Figure 7).

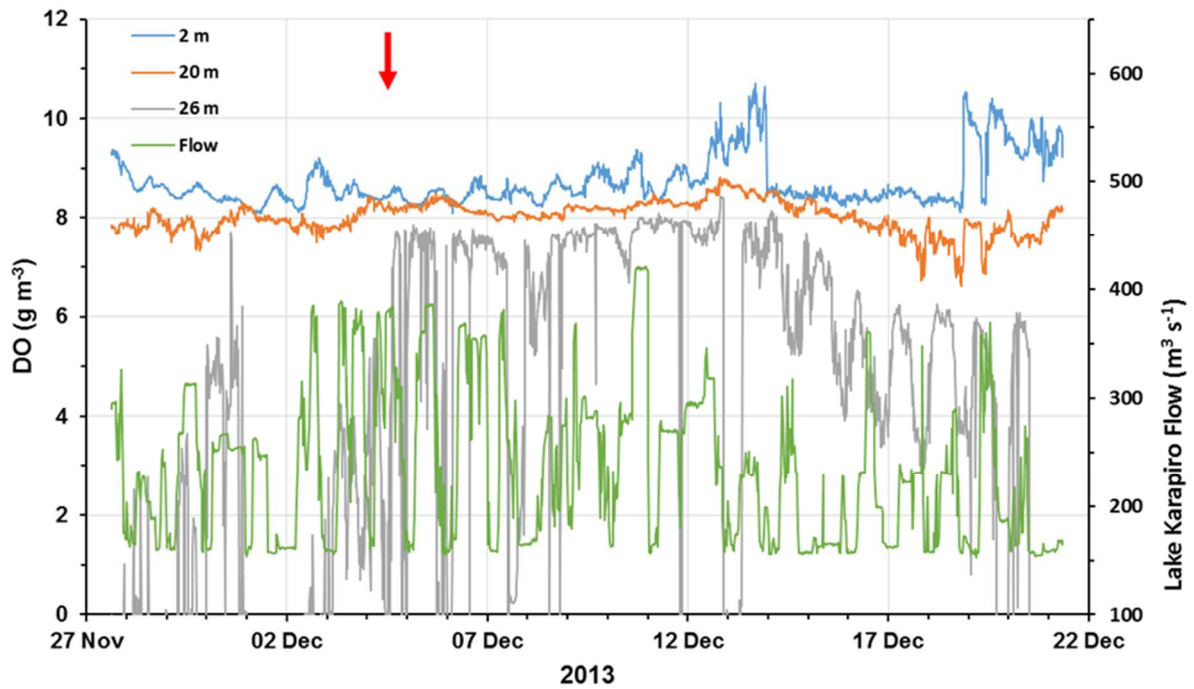


Figure 9: Time-series dissolved oxygen (DO) data at three depths from the thermistor chain relative to flow through Lake Karapiro (right hand axis). DO values $<0.5 \text{ g m}^{-3}$ indicate that the bottom DO probe was in the sediment. Red arrow marks the first sampling visit on 4 December 2013.

Dissolved oxygen data for this period (Figure 9) show that the lake was well oxygenated at 20 m and above. The 26 m depth data shows periodic drops to zero DO. The switching between well oxygenated to anoxic conditions was caused by small changes in water level in the lake allowing the DO sensor to contact the sediment at low level and be lifted out at high level (Figure 10). However, during extended periods with thermal stratification (ΔT) >0.5 °C, bottom water anoxia was also detected. This implies that any anoxic zone in Lake Karapiro at the buoy site must be less than 1 m thick as the thermistor chain was in 27 m water depth. Lake level fluctuations are typically less than 1 m over the day-night cycle of power generation.

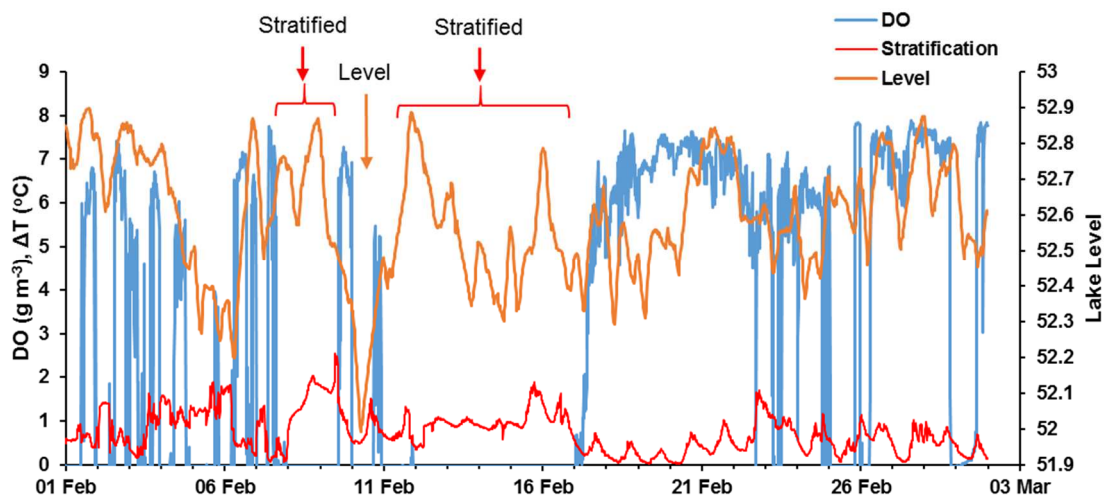


Figure 10: Time series of bottom DO, thermal stratification (ΔT) and lake level in February 2014. Small changes in lake level can move the bottom DO sensor in and out of the anoxic sediment (Figure 9). However, extended periods of thermal stratification, as indicated by ΔT , can result in a thin layer of bottom water anoxia appearing above the sediment. Examples of stratified and level effect anoxia are marked, e.g., between 11 and 17 February the DO above the lake bed was zero due to near bottom stratification. At other times the with zero DO, the probe was in the sediment.

Temperature and DO data from January to April 2014 (Figure 11) show similar patterns to those found in December 2013 (Figure 8). Thermal stratification occurred on a day-night cycle with short periods when the water column remained thermally stratified for several days in mid-summer. This pattern of thermal stratification appeared to be correlated with discharge from Lake Karapiro, with lower discharges resulting in higher day time surface water temperatures than when the discharges were high. The grey loops below the main temperature curves (Figure 11, upper) are the temperature data from the 26 m DO logger when it was in contact with the lake sediment.

The high day time water temperatures and DO concentrations in the upper 2 m during the extended period of low flow from early March to mid-April 2014 are consistent with bright sunny days and the proliferation of hornwort along the sides of the lake. The drop in temperature and DO on 14 March coincided with dull, rainy conditions, which prompted an extra release of water from the lake for power generation (Figure 11).

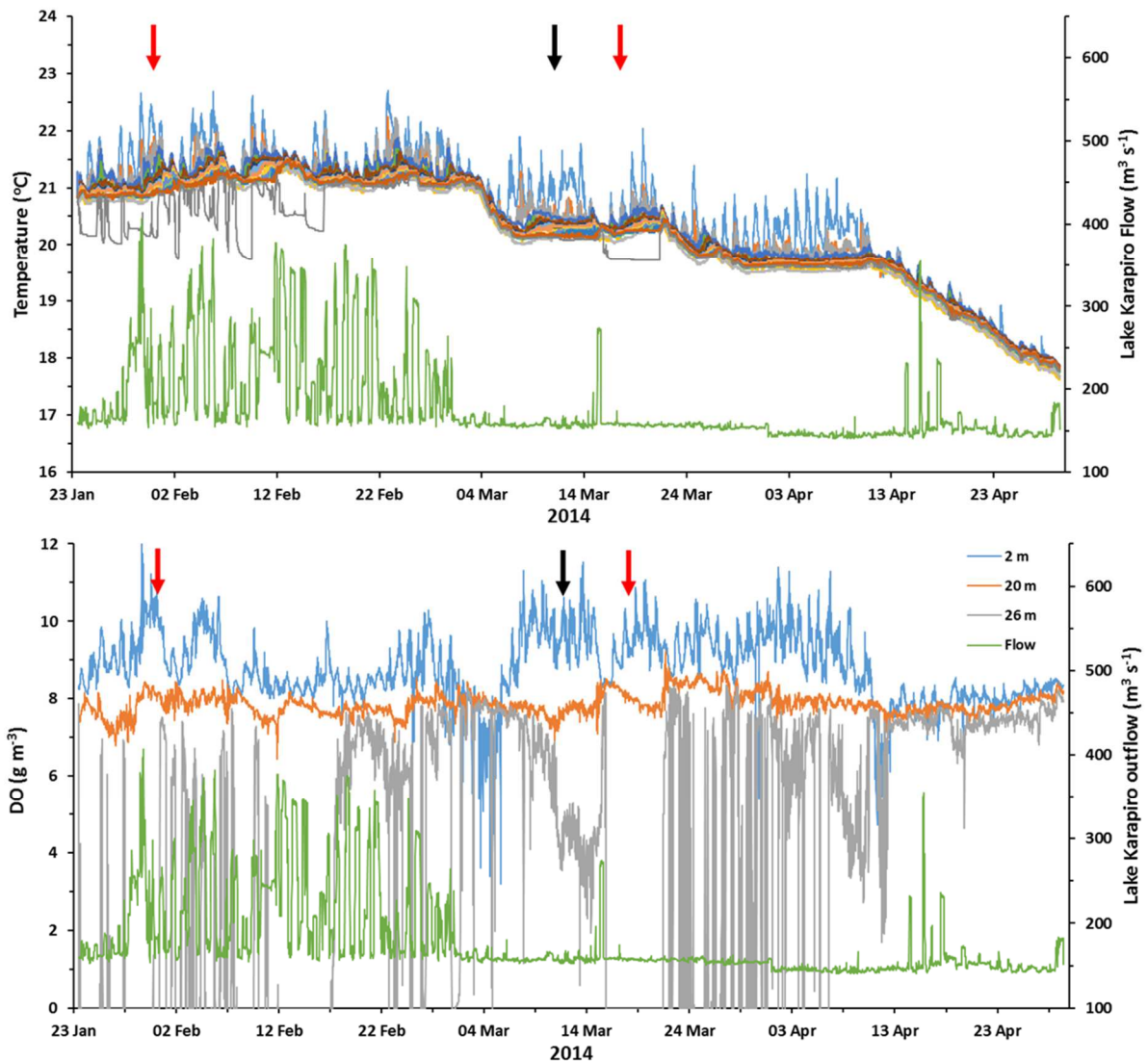
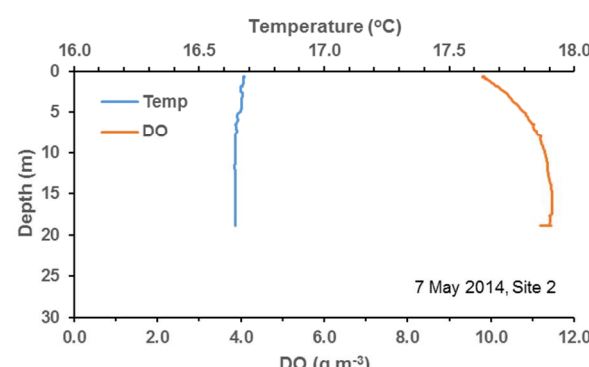
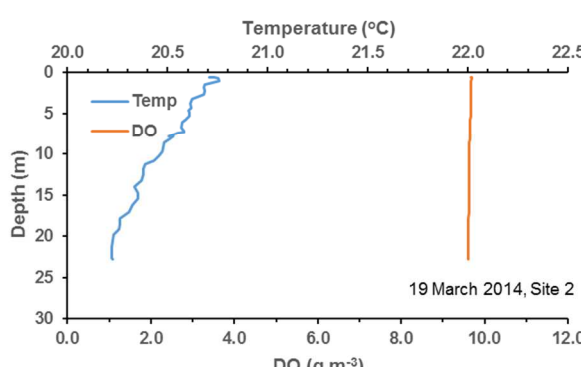
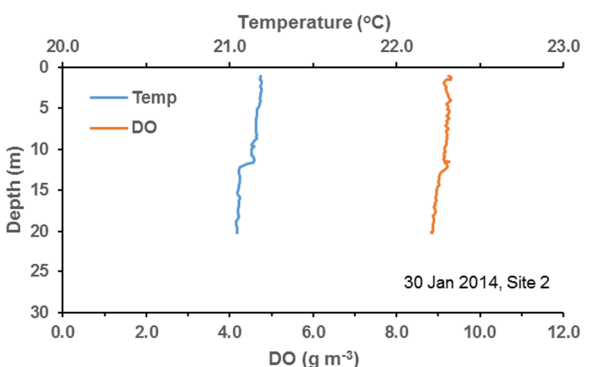
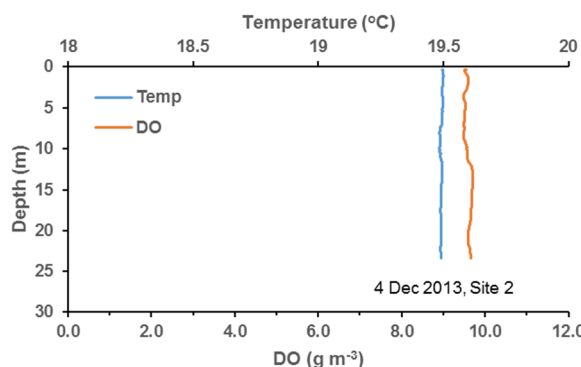
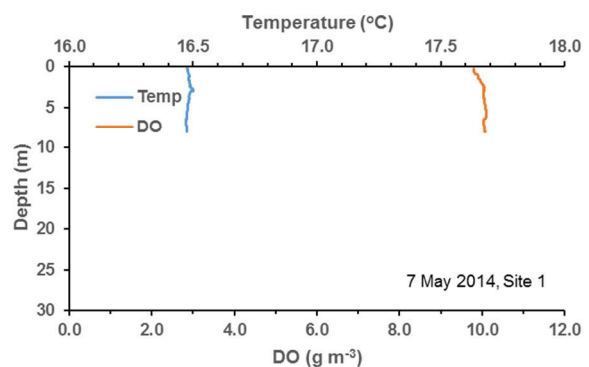
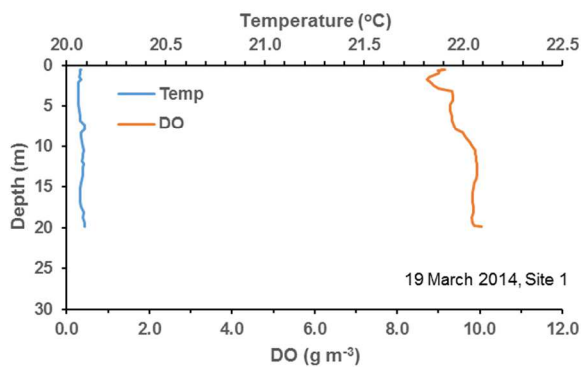
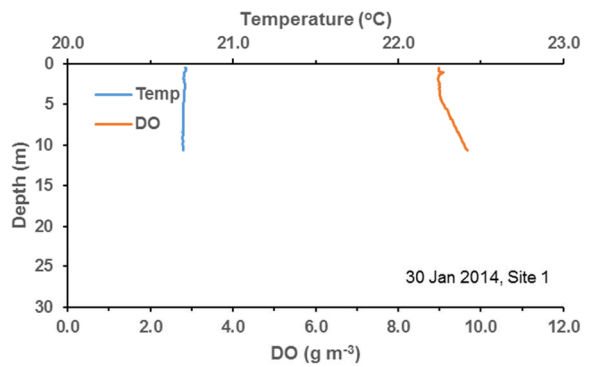
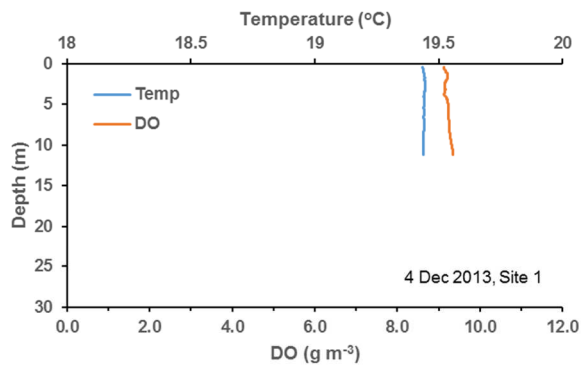
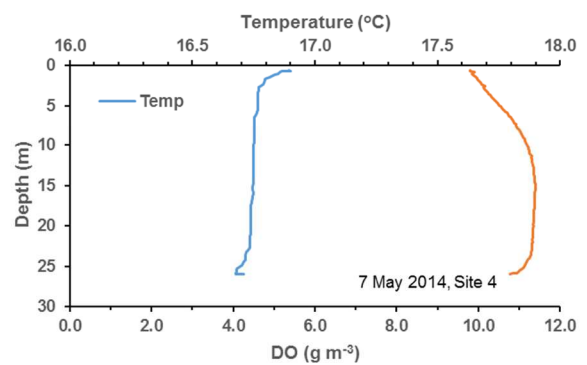
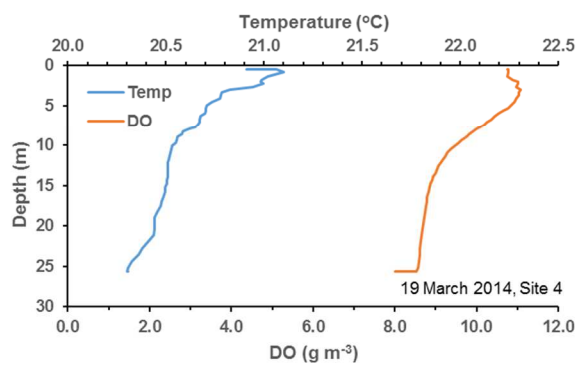
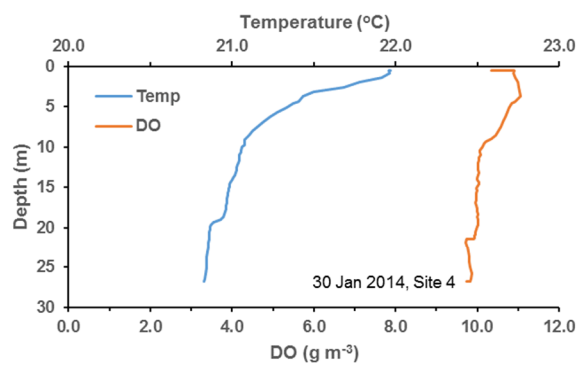
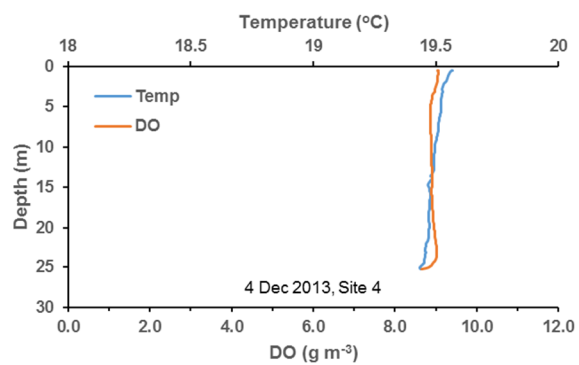
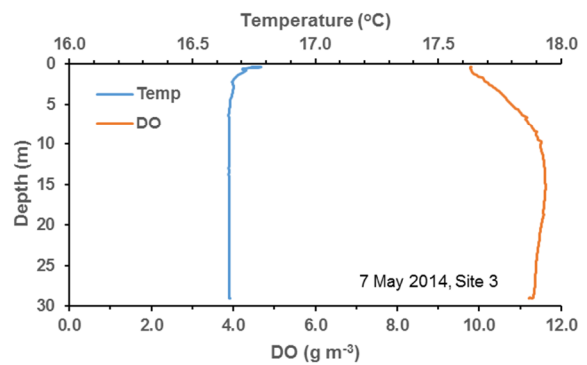
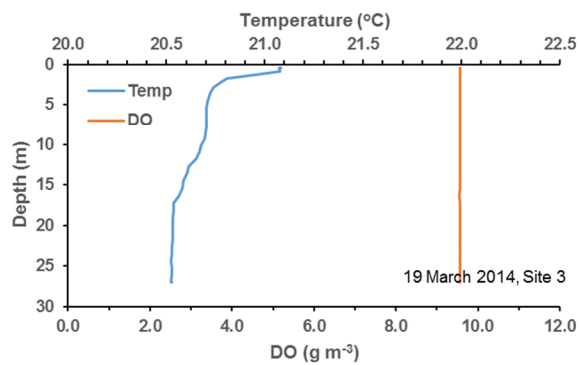
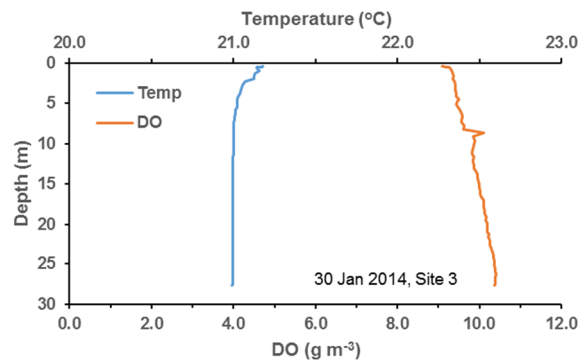
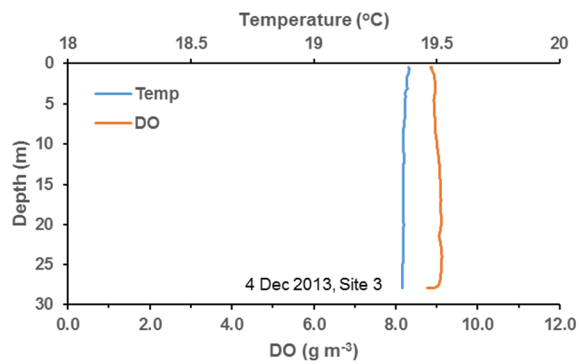


Figure 11: Time-series temperature (upper) and dissolved oxygen (lower) data from the thermistor chain relative to flow through Lake Karapiro (right hand axis) from January to April 2014. Red arrows mark the sampling visits on 30 January and 19 March. The black arrow marks the ADCP current measuring survey visit.

Temperature and DO profiles measured at the individual sites on each occasion (Figure 12) confirmed that the water column was essentially fully oxygenated to the lake bed at each site and on each occasion, with one exception. There was strong thermal stratification with oxygen depletion below the thermocline at site 5 on 4 December 2013 measurements (Figure 12). The layer was less than 3 m thick and was associated with a cold underflow of water from Lake Arapuni. The location of this ‘pool’ of colder water near the Karapiro dam suggests that it may have been there for some time, which would account for the low oxygen.

These profile data do not preclude the existence of low oxygen water at other locations on other occasions but imply that any such layer is likely to have been less than 0.5 m thick, which is the distance of the DO sensor from the bottom of the profiler frame. There was a hint of oxygen depletion at site 4 on 19 March 2014 (Figure 12). This coincides with a period of thermal stratification (Figure 7).





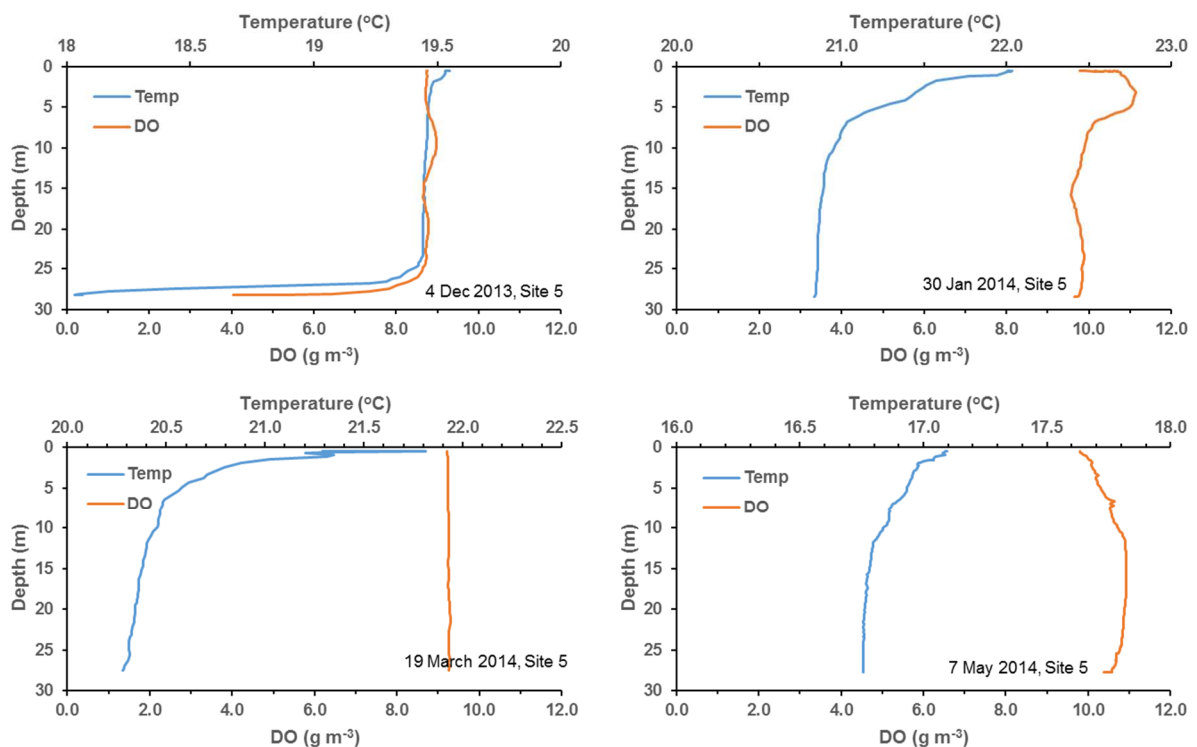


Figure 12: Temperature and DO profiles at individual sites on the four incubation dates. Temperature profiles show surface warming in January and March 2014 at sites downstream from site 2 and only show low oxygen at site 5 in December 2013. The unusual DO profiles in the May data set may indicate DO probe failure.

3.3 Water quality

3.3.1 Nutrients

The nutrient data from the four sampling occasions (Table 3) show temporal and spatial variability, as well as substantial differences between the upper and lower water column.

Total P concentrations in the upper 5 m of water column were less variable between sampling sites than TN but both TP and TN concentrations showed considerable variability at each site between visits (Figure 13).

Total Phosphorus and TN concentrations were essentially the same in the upper 5 m as in the bottom water implying that the water column was mixed. However, DRP concentrations were higher in the bottom waters than in the upper 5 m on three of the sampling visits (Figure 14). In May there was no difference between upper and bottom water concentrations, consistent with the water column being mixed.

There was a similar pattern in the nitrate data (Figure 15) although the separations between upper 5 m water column and bottom water concentrations mainly occurred in January and March 2014.

These data appear to show nutrient reduction in the upper 5 m of water column rather than an increase in nutrient concentrations in the bottom water. This is consistent with increased chlorophyll *a* concentrations in the upper 5 m of water column on those occasions (Section 3.3.2).

Table 3: Nutrient data from the five monitoring sites and the upstream source water from Lake Arapuni on the four sampling occasions. High suspended solids (SS), TP and TN concentrations in the bottom water at site 1 on 4 December 2013 are attributable to bed resuspension under the high flow conditions at that time.

<i>NWA ID</i>	<i>Client ID</i>	<i>SS g/m³</i>	<i>VSS g/m³</i>	<i>Inorg SS</i>	<i>DRP mg/m³</i>	<i>TP mg/m³</i>	<i>NH₄-N mg/m³</i>	<i>NO₃-N mg/m³</i>	<i>TN mg/m³</i>	<i>Chla mg/m³</i>	<i>TN:TP ratio</i>	<i>SD (m)</i>
	4/12/2013											
LI1	Arapuni Tailrace	3.6	1.4	2.3	11	30	40	97	307	7.9	10.2	
LI2	Site 1 Top	3.9	1.3	2.7	11	34	38	114	358	7.9	10.5	2.6
LI3	Site 2 Top	5.1	1.5	3.6	12	34	41	131	378	7.8	11.1	2.4
LI4	Site 3 Top	4.3	1.2	3.1	15	35	47	156	393	6.8	11.2	2.85
LI5	Site 4 Top	3.1	1.0	2.1	14	32	46	167	392	6.4	12.3	2.7
LI6	Site 5 Top	3.1	1.0	2.1	15	33	50	163	389	6.3	11.8	2.7
LI7	Site 1 Bottom	25.3	4.2	21.1	14	77	44	118	533	9.8	6.9	
LI8	Site 2 Bottom	5.1	1.3	3.8	14	37	43	129	356	7.3	9.6	
LI9	Site 3 Bottom	5.3	1.2	4.1	16	41	47	153	387	6.2	9.4	
LI10	Site 4 Bottom	3.8	0.9	3.0	17	39	75	176	409	4.1	10.5	
LI11	Site 5 Bottom	3.4	0.9	2.5	17	37	60	165	388	4.5	10.5	
	30/01/2014											
NR1	Arapuni Tailrace	4.0	1.6	2.4	4	28	18	38	282	9.8	10.1	
NR2	Site 1 Top	4.0	1.6	2.4	6	30	18	73	318	8.3	10.6	2.5
NR4	Site 2 Top	3.6	1.3	2.3	5	32	12	69	355	7.9	11.1	2.4
NR6	Site 3 Top	3.7	1.8	1.9	4	33	19	67	487	11.1	14.8	2.2
NR8	Site 4 Top	4.3	2.2	2.1	3	35	5	10	342	20.2	9.8	2.4
NR10	Site 5 Top	3.8	2.1	1.7	3	34	7	9	342	18.9	10.1	2.4
NR3	Site 1 Bottom	4.1	1.7	2.4	7	32	26	75	379	8.1	11.8	
NR5	Site 2 Bottom	4.2	1.5	2.7	8	32	30	79	338	7.6	10.6	
NR7	Site 3 Bottom	4.1	1.5	2.6	6	32	21	72	314	9.1	9.8	
NR9	Site 4 Bottom	3.3	1.1	2.2	10	32	38	100	333	6.8	10.4	
NR11	Site 5 Bottom	3.4	1.0	2.4	12	36	39	110	337	6.3	9.4	
NR12	Karapiro 30m				14		57	111				
	19/03/2014											
QP1	Arapuni Tailrace	3.4	1.2	2.2	6.3	28	8	45	217	13.4	7.8	
QP2	Site 1 Top	3.6	1.3	2.3	8.8	34	14	94	325	11.5	9.6	2.5
QP4	Site 2 Top	3.3	1.6	1.8	2.9	30	4	57	299	22.2	10.0	2.6
QP6	Site 3 Top	4.1	1.9	2.2	2.5	32	4	59	326	23.3	10.2	2.3
QP8	Site 4 Top	4.2	2.0	2.1	1.6	31	4	23	306	26.3	9.9	2.6
QP10	Site 5 Top	4.3	2.0	2.4	1.6	28	3	31	280	25.0	10.0	2.2
QP3	Site 1 Bottom	3.0	1.0	2.0	9.2	30	15	98	308	10.5	10.3	
QP5	Site 2 Bottom	3.5	1.1	2.4	8.6	33	25	114	321	11.8	9.7	
QP7	Site 3 Bottom	4.8	1.4	3.4	5.6	31	17	85	321	15.4	10.4	
QP9	Site 4 Bottom	3.4	0.9	2.5	9.8	31	45	92	319	9.1	10.3	
QP11	Site 5 Bottom	3.0	0.9	2.2	9.7	31	40	88	295	9.0	9.5	
	7/05/2014											
SV1	Arapuni Tailrace	1.9	0.7	1.1	20	33	12	240	373	4.1	11.3	
SV2	Site 1 Top	3.2	1.1	2.1	22	39	20	274	460	4.2	11.8	2.3
SV4	Site 2 Top	2.6	0.8	1.8	22	36	15	307	453	4.1	12.6	2.4
SV6	Site 3 Top	2.2	0.8	1.4	21	35	15	295	446	4.5	12.7	2.4
SV8	Site 4 Top	2.3	0.8	1.5	21	34	13	287	431	5.6	12.7	2.5
SV10	Site 5 Top	2.2	1.0	1.2	17	34	6	247	418	7.5	12.3	2.4
SV3	Site 1 Bottom	2.6	0.7	1.9	22	35	17	271	425	3.4	12.1	
SV5	Site 2 Bottom	2.6	0.7	1.8	22	37	18	305	448	3.9	12.1	
SV7	Site 3 Bottom	2.5	0.7	1.7	22	35	20	294	448	3.7	12.8	
SV9	Site 4 Bottom	1.8	0.7	1.2	21	34	17	288	426	3.7	12.5	
SV11	Site 5 Bottom	3.9	0.8	3.1	21	37	24	283	438	3.1	11.8	

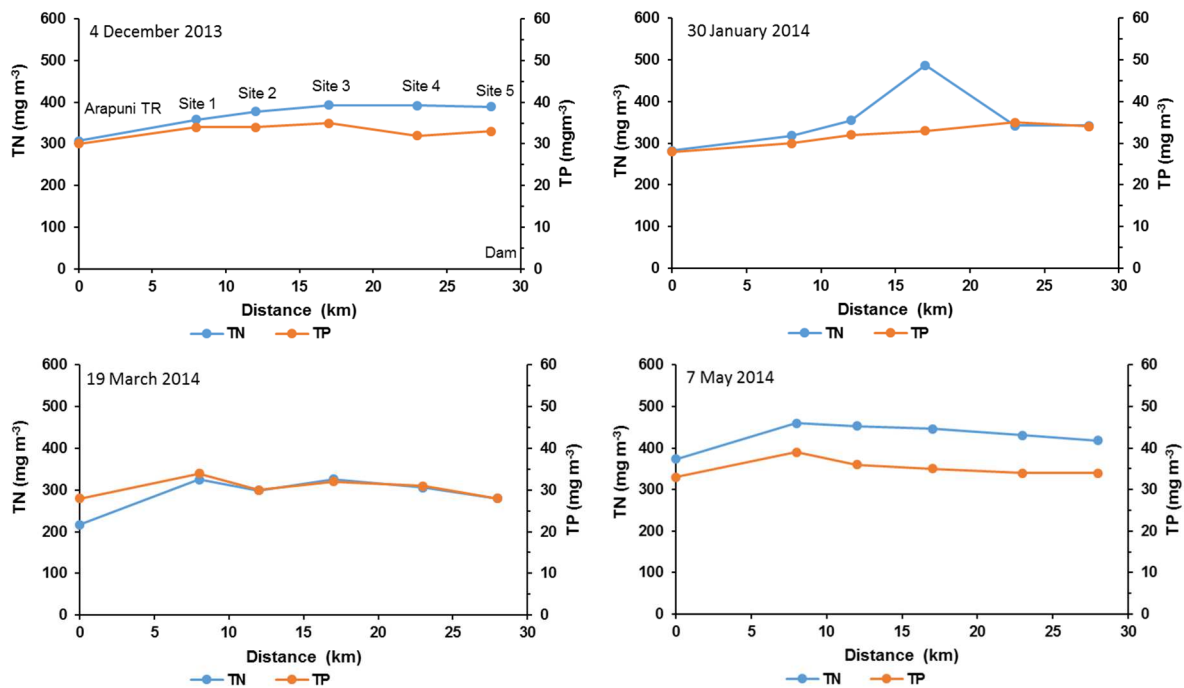


Figure 13: Upper water column TN and TP concentrations on the four sampling occasions. Site names are as per the 4 December 2013 graph. Distance is the estimated distance in km below the Lake Arapuni discharge at 0 km.

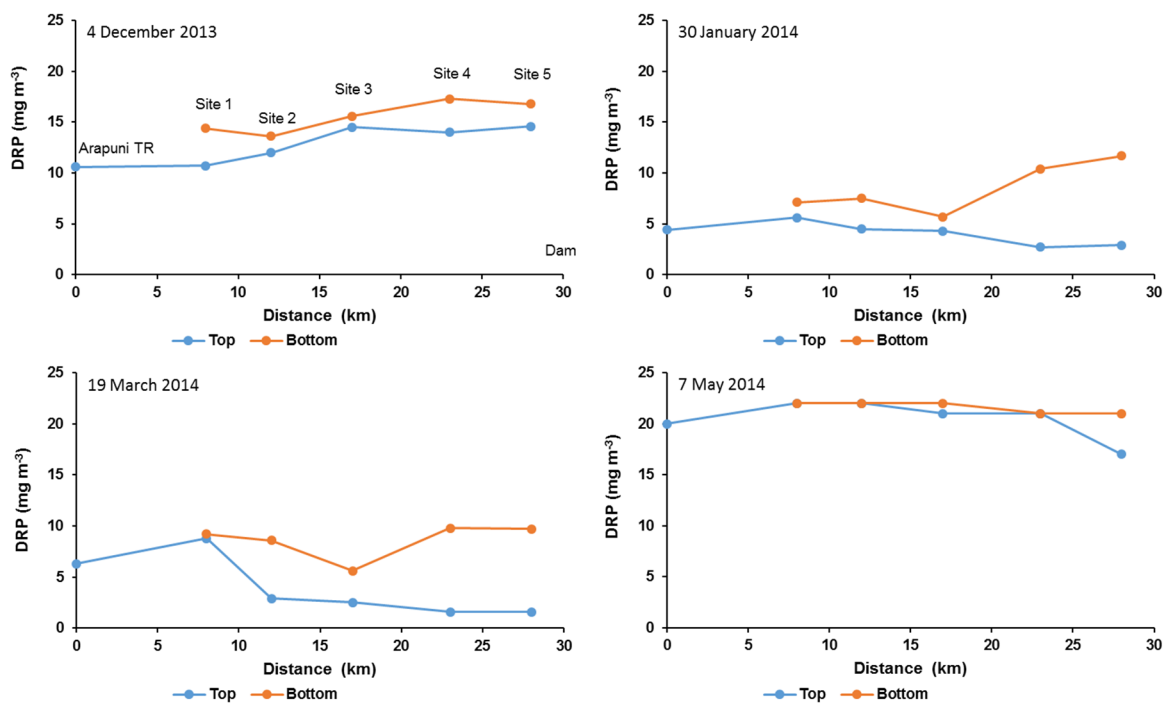


Figure 14: Dissolved reactive phosphorus (DRP) concentrations in the upper 5 m and bottom water at each site on each occasion. Site names are as per the 4 December 2013 graph. Distance is the estimated distance in km below the Lake Arapuni discharge at 0 km.

Ammonium ($\text{NH}_4\text{-N}$) concentrations increased in the bottom waters with increasing distance downstream (Figure 16). These increases imply anoxic conditions at the sediment surface preventing nitrification or that the efflux of $\text{NH}_4\text{-N}$ from the anoxic sediments exceeded the nitrification rate. In general $\text{NH}_4\text{-N}$ concentrations decreased in the surface waters between sampling dates rather than increased in the bottom waters, again consistent with increased chlorophyll a concentrations in the upper 5 m of water column (Section 3.3.2).

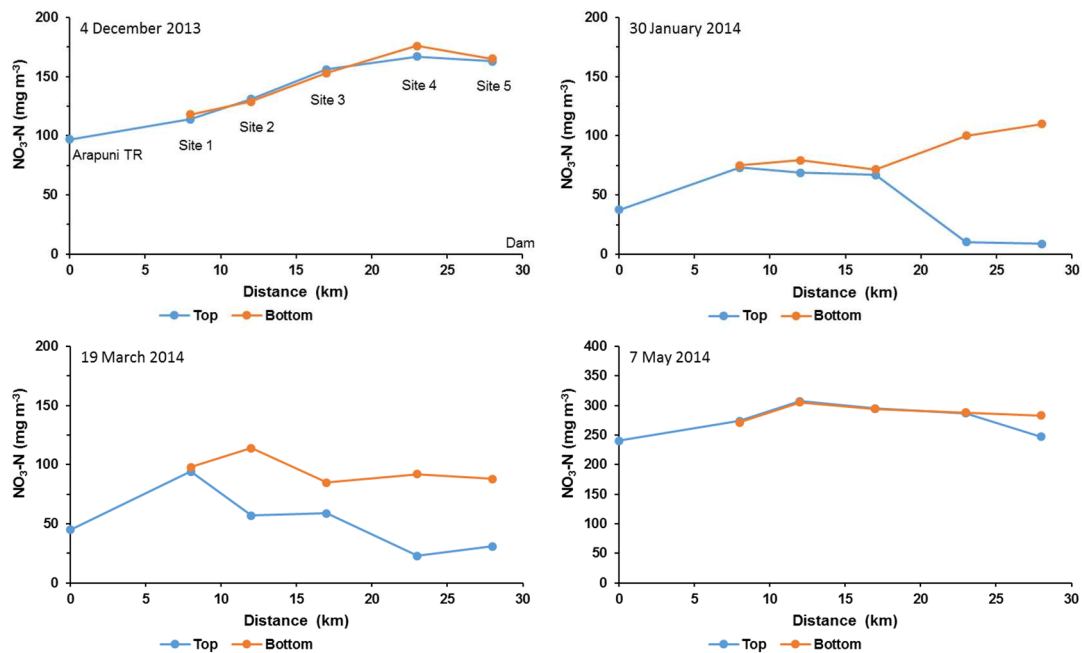


Figure 15: Nitrate nitrogen ($\text{NO}_3\text{-N}$) concentrations in the upper 5 m and bottom water at each site on each occasion. Site names are as per the 4 December 2013 graph. Distance is the estimated distance in km below the Lake Arapuni discharge at 0 km. Note different vertical axis scale on the May graph.

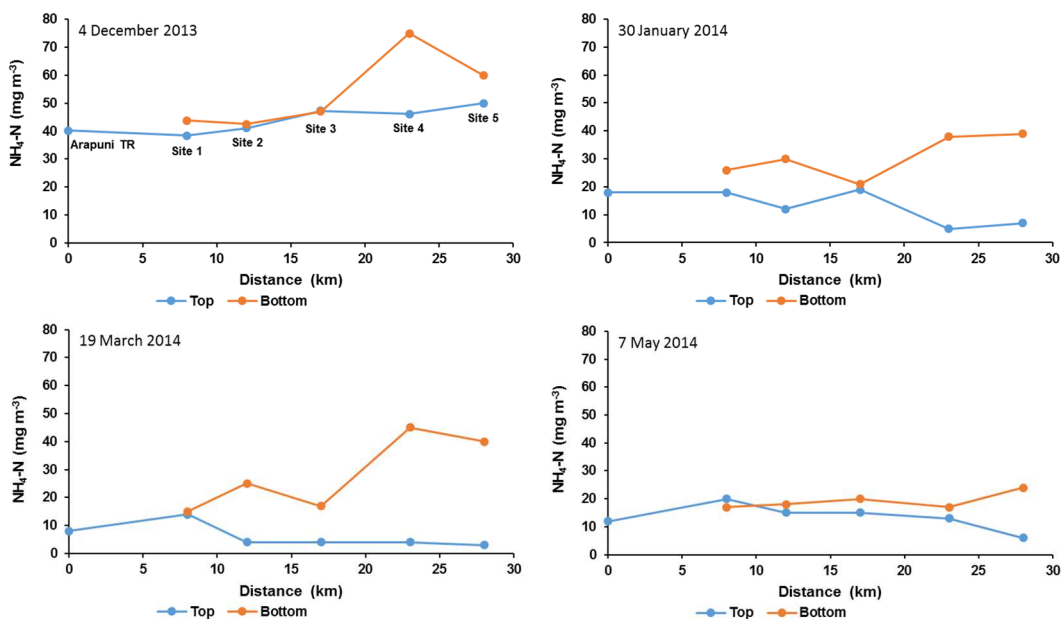


Figure 16: Ammonium ($\text{NH}_4\text{-N}$) concentrations in the upper 5 m and bottom water at each site on each occasion. Site names are as per the 4 December 2013 graph. Distance is the estimated distance in km below the Lake Arapuni discharge at 0 km.

3.3.2 Chlorophyll-a

In December 2013 (Figure 17), chlorophyll *a* concentrations were generally less than 10 mg m⁻³ at all sites and the temperature was uniform, except at site 5 where there was cold water on the bottom (Figure 18), most likely the remnant of the underflowing cold water from Lake Arapuni.

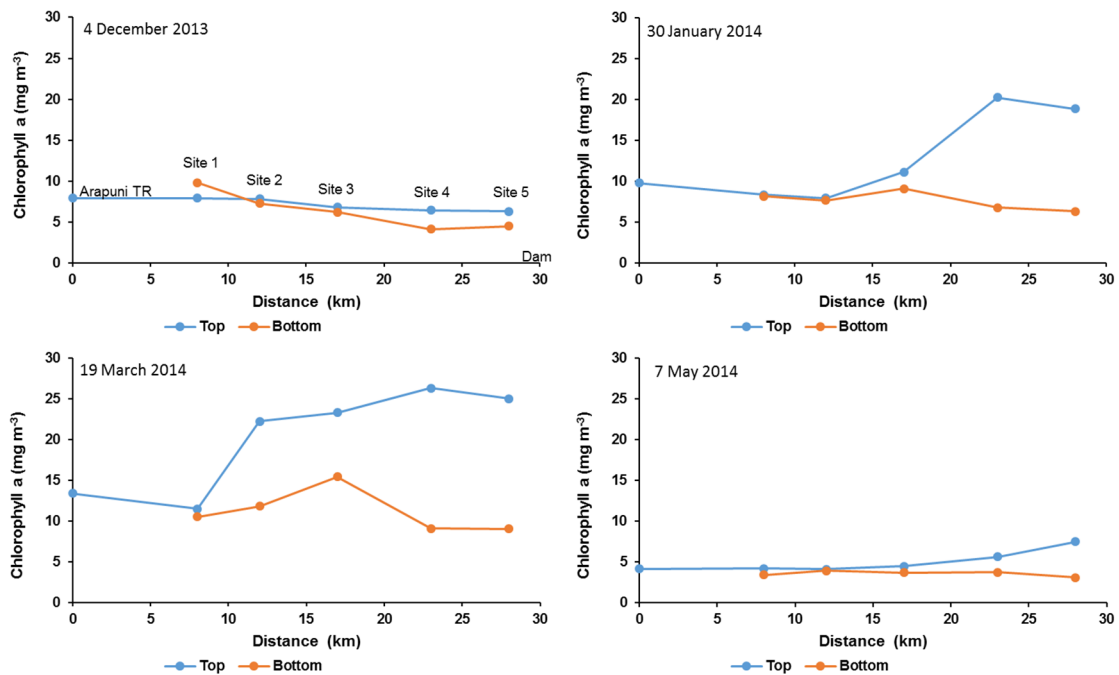


Figure 17: Chlorophyll *a* concentrations in the upper 5 m and bottom water at each site on each occasion. Site names are as per the 4 December 2013 graph. Distance is the estimated distance in km below the Lake Arapuni discharge at 0 km.

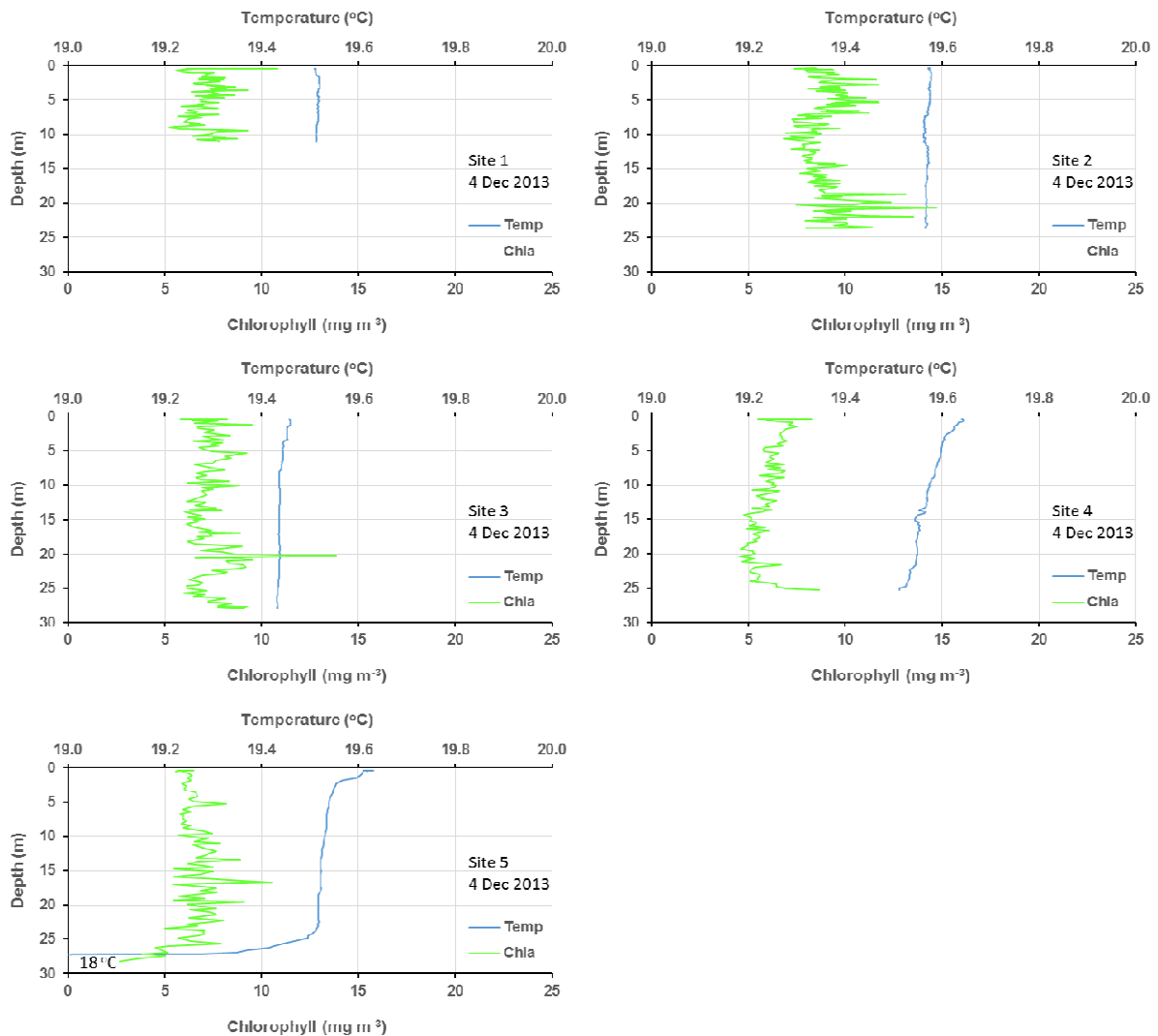


Figure 18: Depth profiles of temperature and chlorophyll at each site in December 2013.

In January 2014, chlorophyll *a* concentrations were higher than in December. There was a pronounced increase in chlorophyll *a* concentrations in the upper water column above about 8 m from site 4 through to site 5 (Figure 19). These higher chlorophyll *a* concentrations coincided with an apparent thermal stratification in the upper water column and are consistent with observations from the water quality data.

Chlorophyll *a* concentrations in March 2014 (Figure 20) were similar to those in January but with the elevated upper water column chlorophyll *a* concentrations also occurring at sites 2 and 3. It is likely that the elevated upper water column chlorophyll *a* concentrations developed because of the thermal stratification, which would confine the phytoplankton in the high light zone for maximum growing time, and the low flow through Lake Karapiro, which would increase their residence time allowing them to utilise the available nutrients in the upper water column. This is consistent with the observation that phytoplankton may have run out of nutrients in the nutrient addition and zooplankton dilution experiments (see Section 3.5).

In May 2014, temperature and light levels had fallen substantially and chlorophyll *a* concentrations were very much lower than in January and March 2014 (Figure 21).

These data suggest that the seasonal growth of phytoplankton in Lake Karapiro is mostly between January and March, inclusive. This is also the time when drought-like climatic conditions prevail such that water discharge through Lake Karapiro is lowest and residence time is highest. A consequence of these maximum growth factors is that nutrient depletion is likely to occur in the upper water column and nutrient limitation may become important.

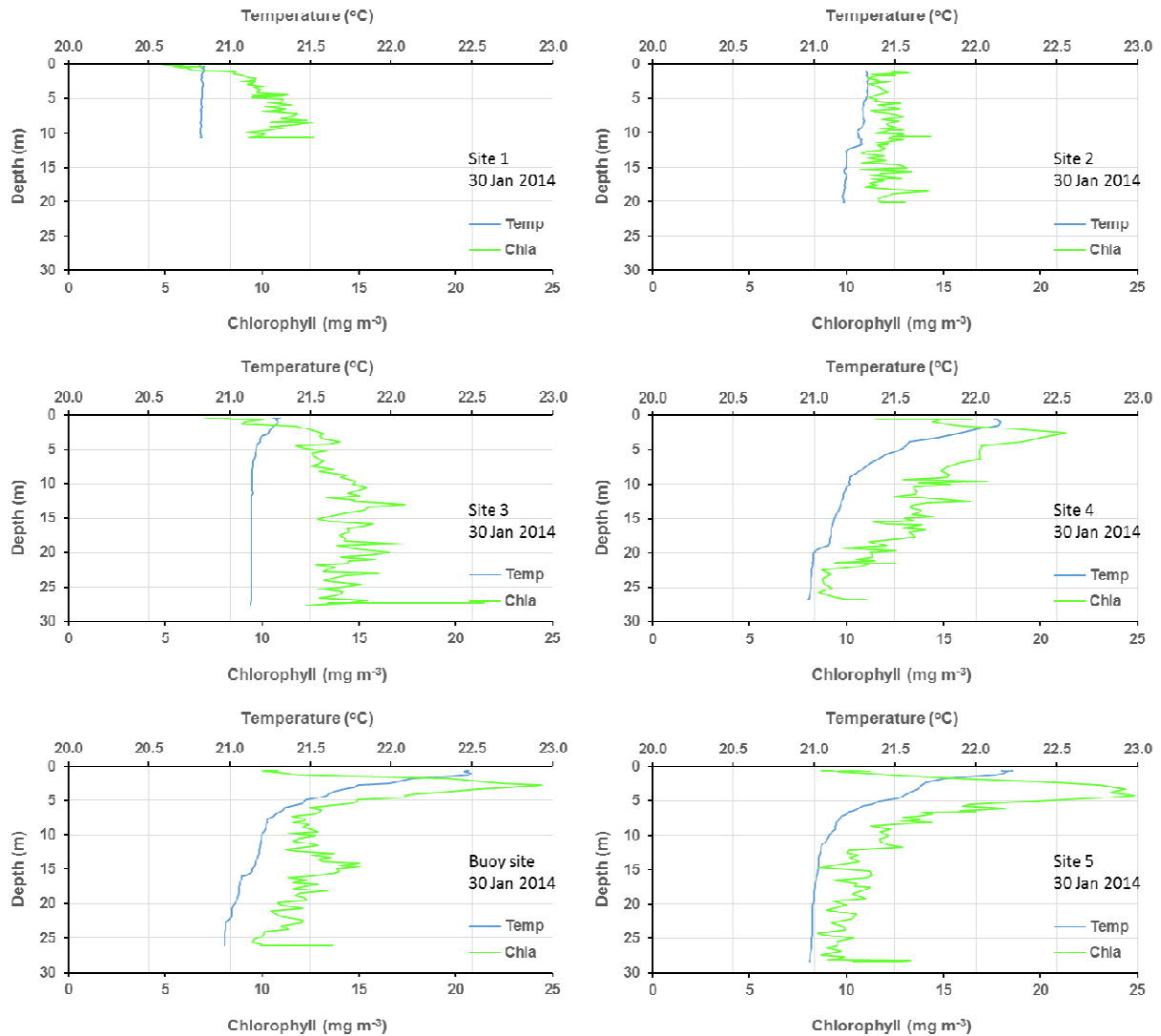


Figure 19: Depth profiles of temperature and chlorophyll at each site in January 2014. Profiles from the buoy site are included in this set to provide more information between sites 4 and 5.

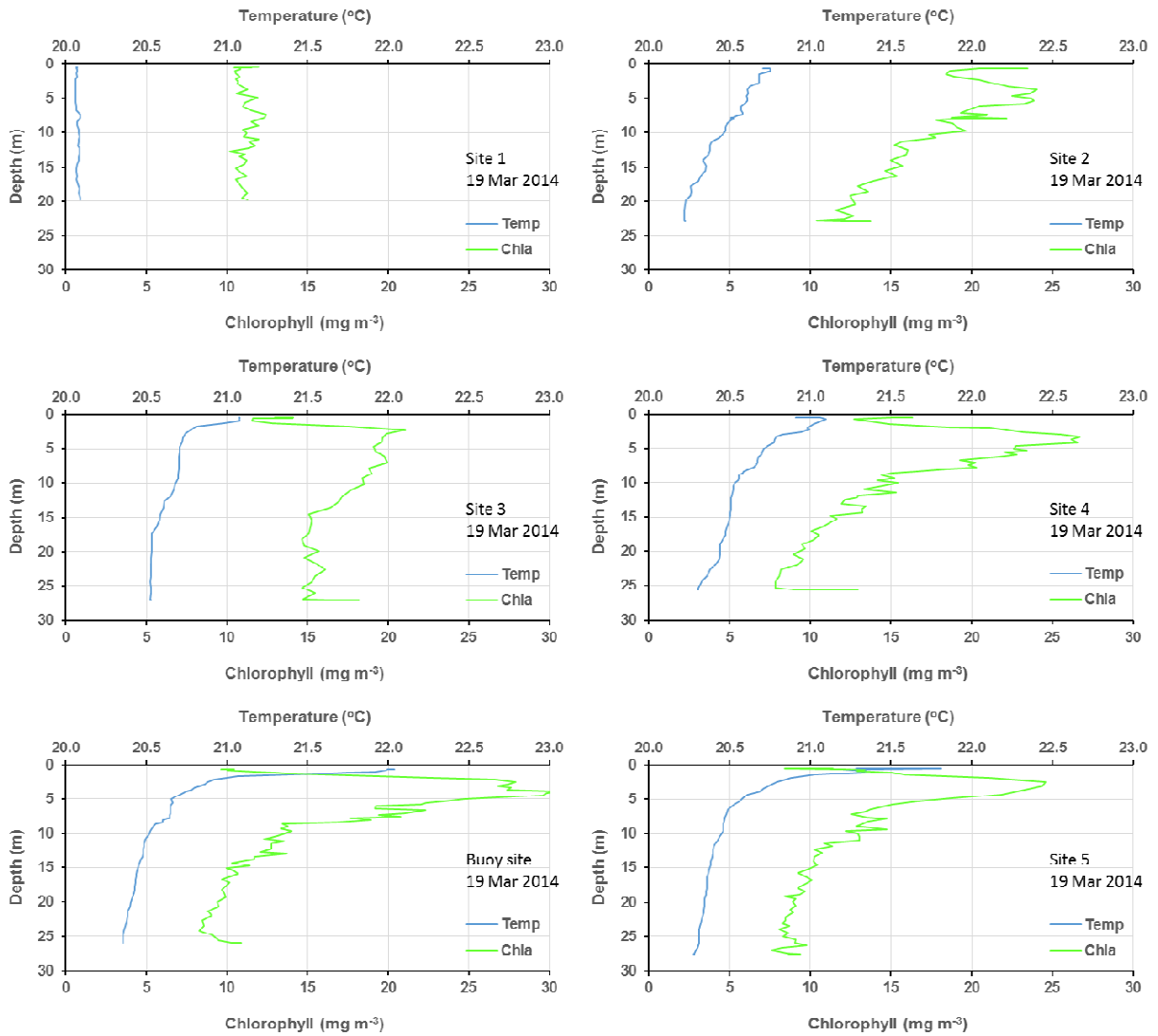


Figure 20: Depth profiles of temperature and chlorophyll at each site in March 2014 . Profiles from the buoy site are included in this set to provide more information between sites 4 and 5.

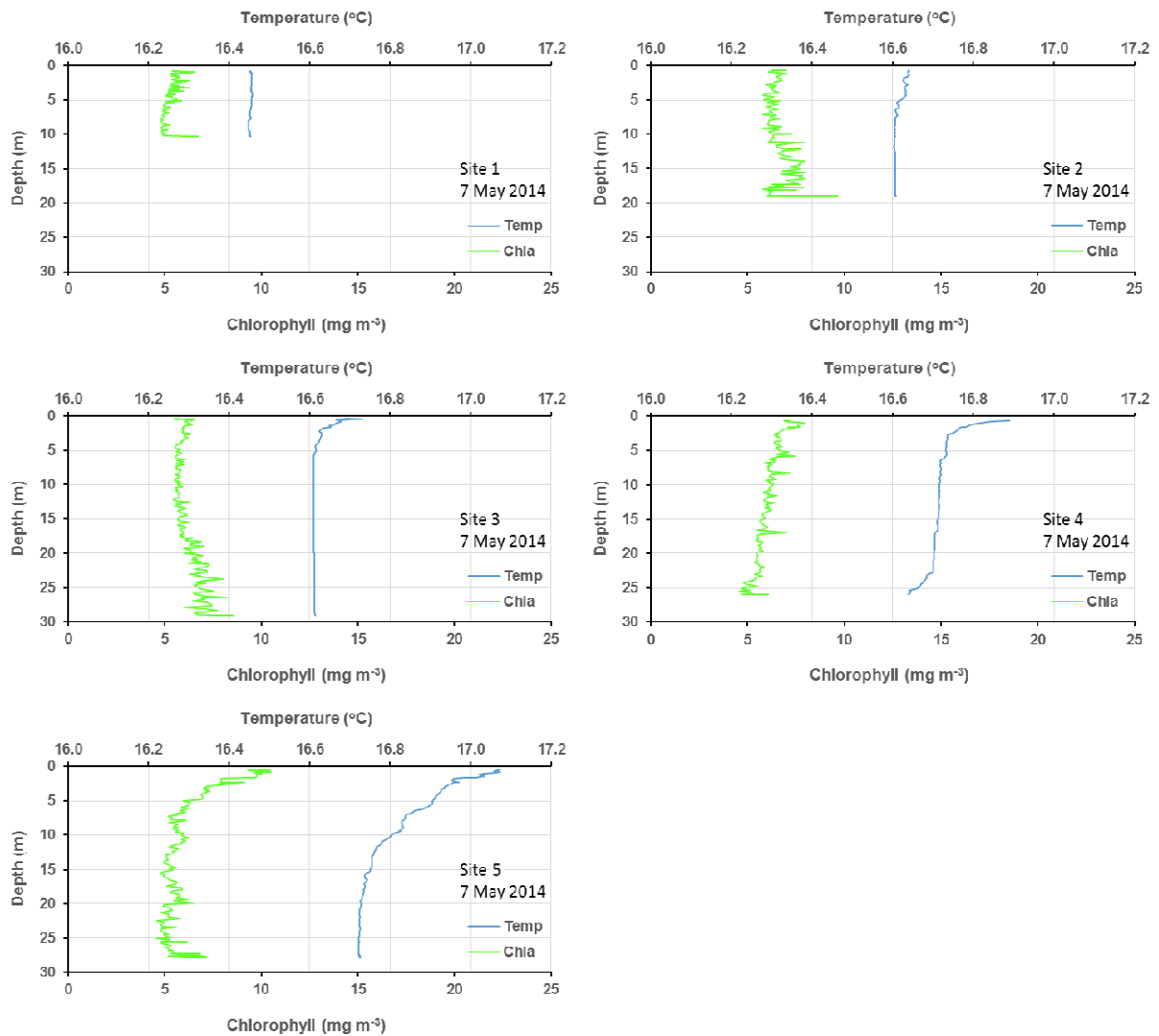


Figure 21: Depth profiles of temperature and chlorophyll at each site in May 2014.

3.4 Phytoplankton and Zooplankton

3.4.1 Phytoplankton

An important factor affecting chlorophyll *a* concentrations in a lake or reservoir is the species composition of the algal assemblage. Phytoplankton species composition in Lake Karapiro in each of the four experiments was dominated by diatoms with similar proportions of flagellates in December 2013 and March 2014 (Figure 22). The main diatom species was *Fragilaria crotonensis* in December 2013 and January 2014, changing to *Attheya sp.* in March 2014 and *Aulacoseira granulata var. angustissima* in May 2014. The flagellates were mostly small unicells (<5 μm) and *Cryptomonas sp.* Desmids had highest biomass in December 2013 and March 2014 and picoplankton had highest biomass in December 2013 and March and May 2014. Cyanobacteria were always present at low biomass except at site 1 in January 2014. Because cyanobacteria require calm water to proliferate, it is almost certain they were from Lake Arapuni upstream.

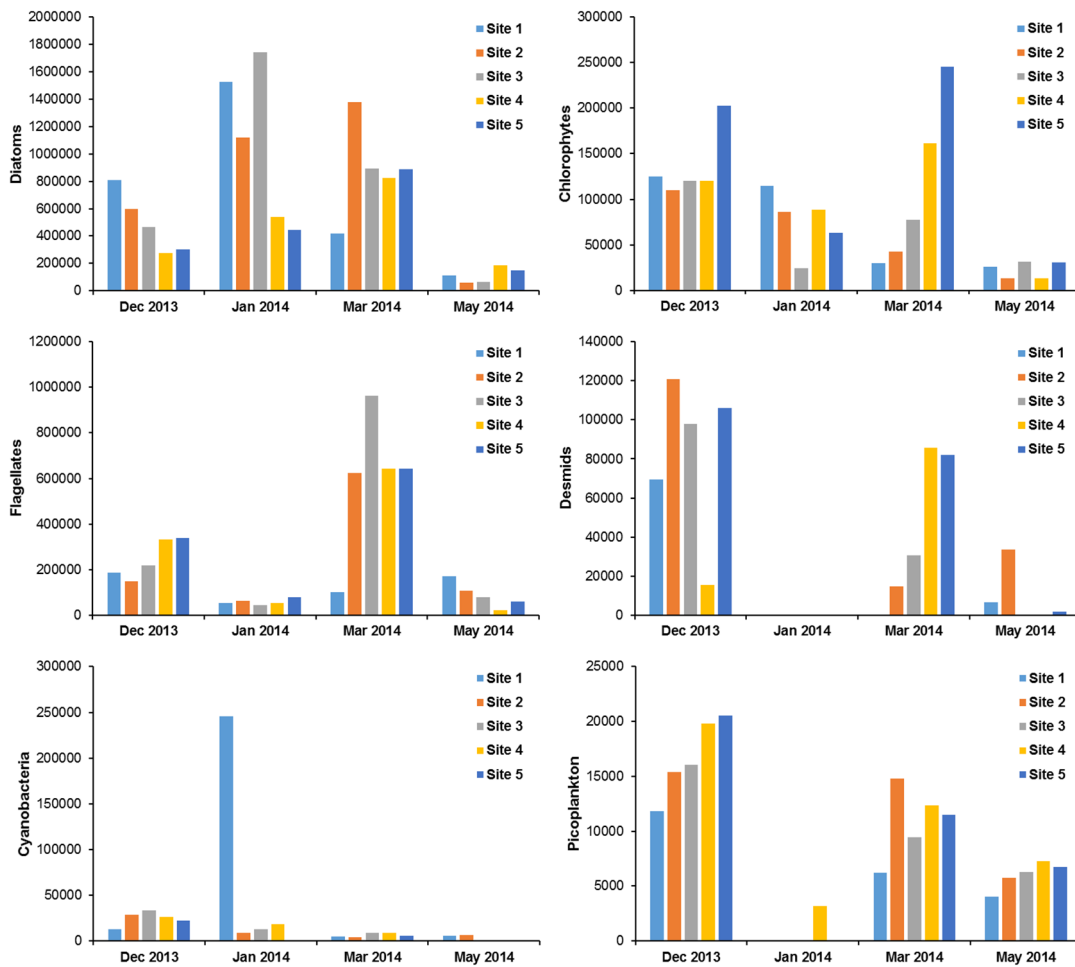


Figure 22: Changes in phytoplankton species composition and abundance between sites and between sampling dates. Flow regimes were high (Dec 13), medium (Jan 14), low stratified (Mar 14) and low mixed (May 14). Data are total biovolume (μm^3). Note the different vertical scales.

3.4.2 Zooplankton

In December 2013, zooplankton species composition was dominated by the Cladocerans, *Bosmina meridionalis* and *Daphnia galeata* (Figure 23). The species composition through January to May 2014 was dominated by rotifers with more copepods in January 2014 than at any other time. Zooplankton biomass was very low through March to May 2014 which may have been a response to the low flow conditions through that period.

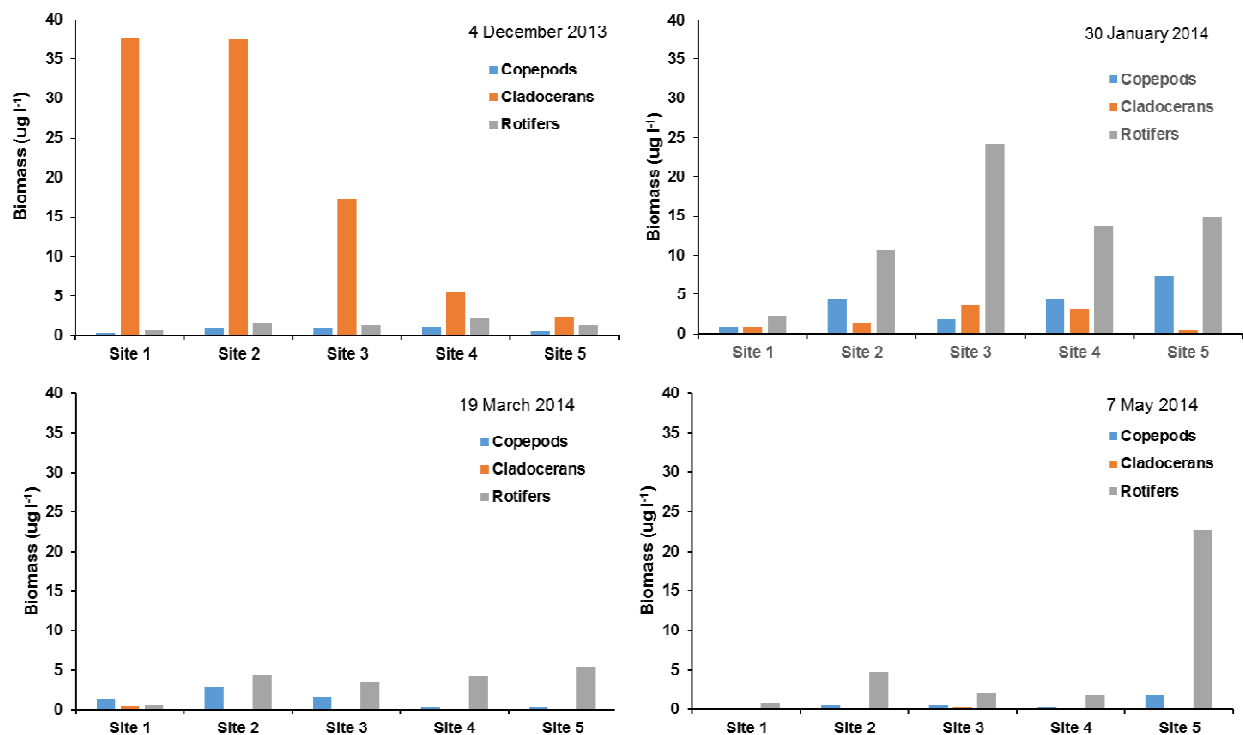


Figure 23: Zooplankton biomass at the five sites on each of the four sampling occasions.

3.5 PPR Bioassays

The PPR bioassay results (Figure 24) show highest net carbon uptake (growth) in the euphotic zone (half Secchi depth) and almost no uptake at two and half times the Secchi depth. These data indicate that light limitation is important below about 6 m depth. Assuming the Secchi depth represents the 5% light level, the phytoplankton were still growing under those low light conditions.

The maximum growth occurred in January and March 2014, consistent with the chlorophyll *a* data (Figure 20). Anomalous low results at site 3 in December 2013 and January 2014 appear to be real and can be explained when considered against the hydrodynamic results (see discussion). The missing data from site 2 and low values for site 1 in May 2014 (Figure 24) are attributable to the effects of drifting weed masses compromising that experiment.

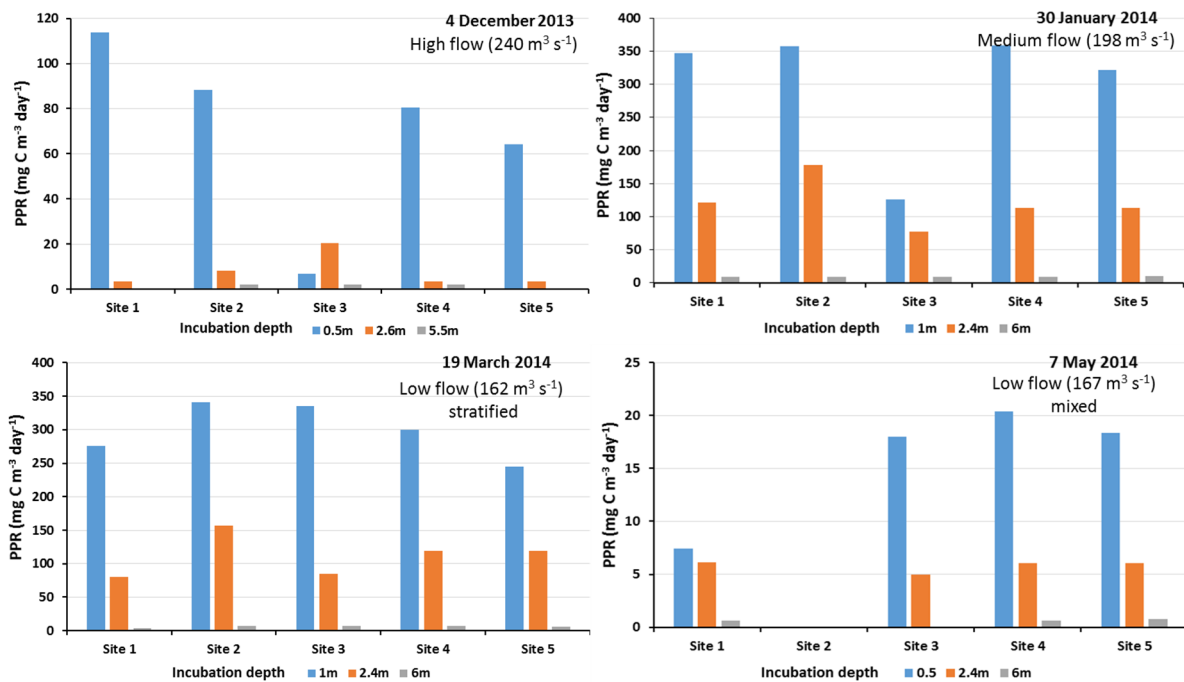


Figure 24: PPR results plotted as net carbon uptake rates in $\text{mg C m}^{-3} \text{d}^{-1}$ for the five sites on each of the four sampling visits. Flow classifications were based on the mean discharge from Lake Karapiro over the seven days before the PPR incubations. The results on 7 May 2014 show the marked effect of weed (site 2 missing) and low light levels in autumn. Note the different vertical scales.

Surface irradiance data (Figure 25) were used in the calculation of PPR net carbon uptake rates. These data show the variable nature of light over a day and the seasonal reduction in PAR between summer and autumn.

Underwater light was recorded as a vertical profile at each site on each occasion. In general, the underwater light field to 1% of near surface irradiance was at less than 10 m depth, even under relatively high clarity (Figure 26). Secchi depth values ranged from 2.2 to 2.85 m (Table 3) giving a lower PPR incubation depth of around 7 m in December 2013.

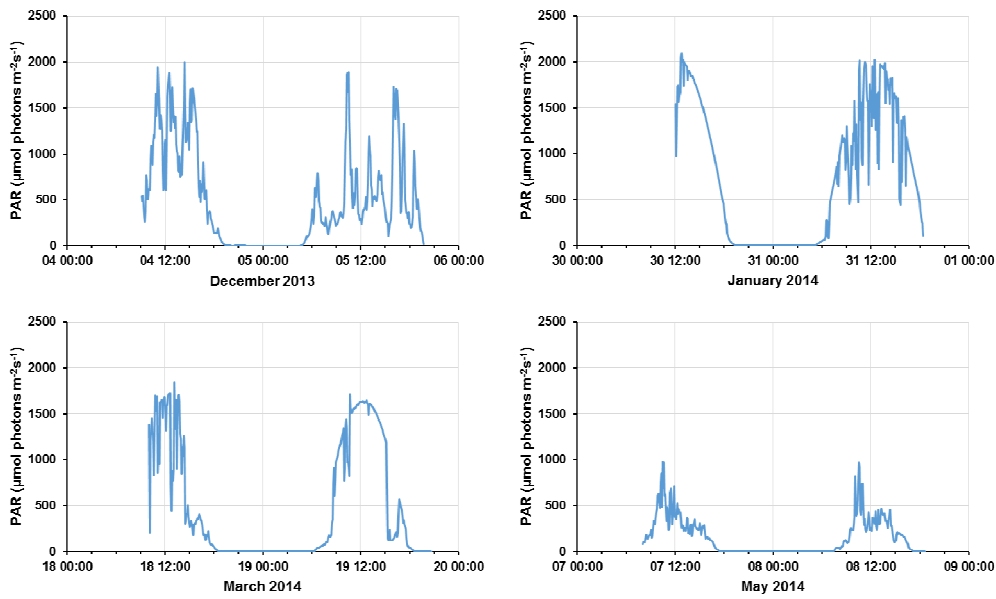


Figure 25: Photosynthetically available radiation (PAR) light records for the four sampling visits. Data recorded at Cambridge over the period of each PPR incubation.

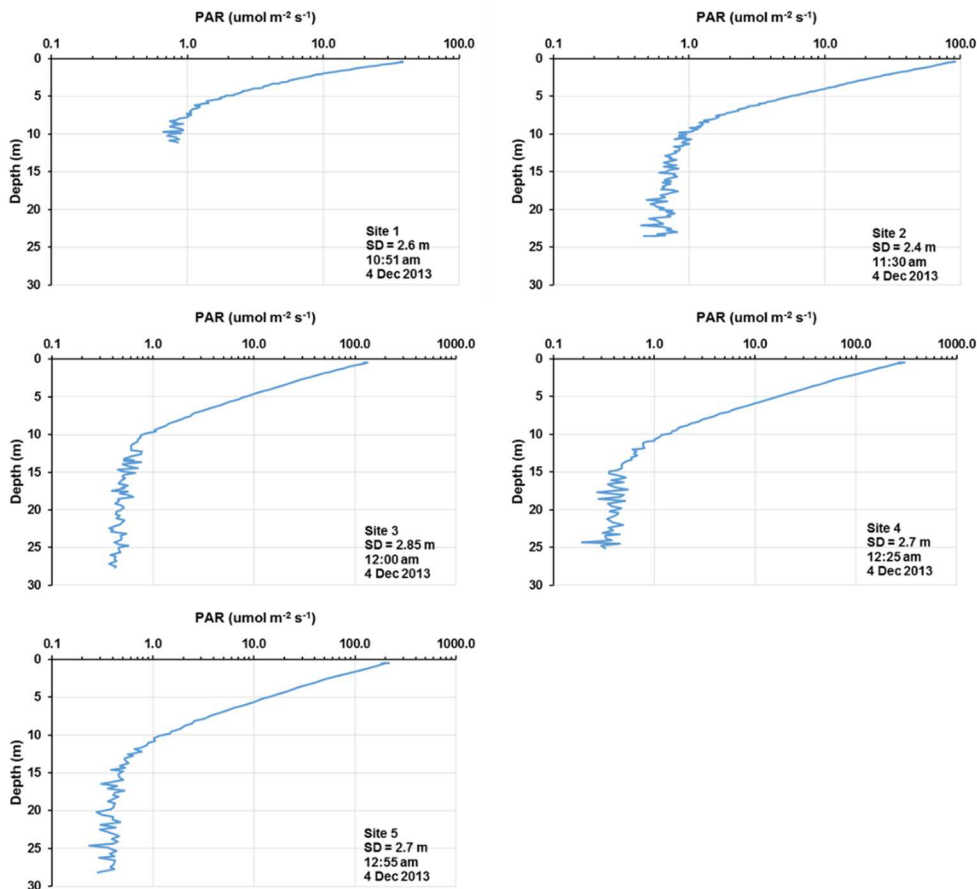


Figure 26: A set of underwater light profiles measured on 4 December 2013. Note different PAR axis at sites 1 and 2. Full dataset from each sampling are held by NIWA and may be available on request with DNZ permission.

3.6 Nutrient addition bioassay

The nutrient addition bioassay (Figure 27, Figure 28) was a one-off experiment in March, to assess whether there was any evidence of nutrient limitation to phytoplankton growth at any of the sampling sites in the lake.

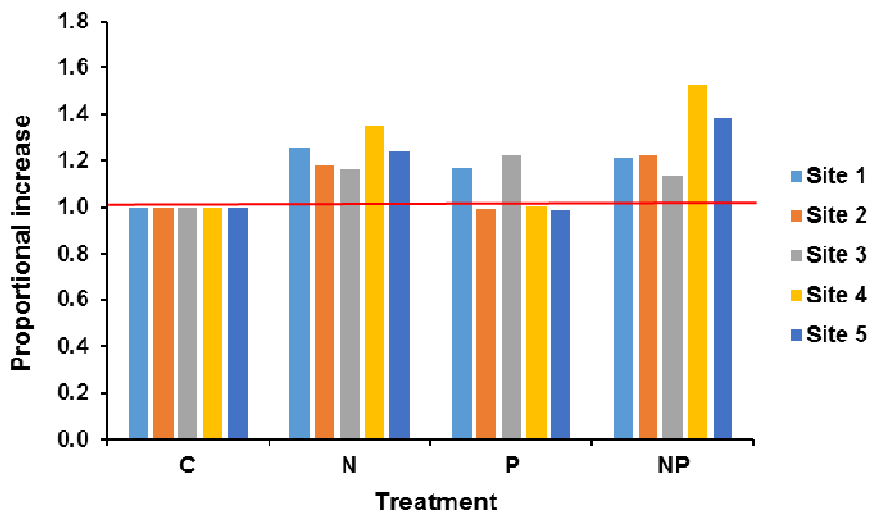


Figure 27: Nutrient addition bioassay results showing the response to the addition of N, P and N+P as a proportional increase relative to the control. Values around 1 indicate no response. Values above 1 indicate a positive response.

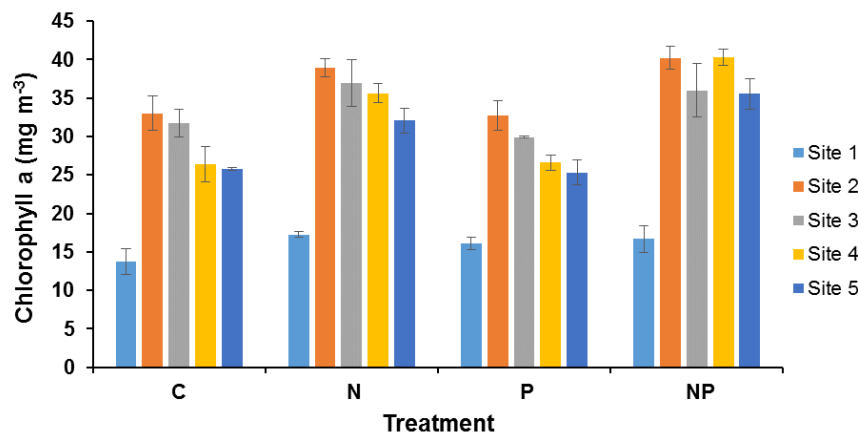


Figure 28: Nutrient addition bioassay results showing chlorophyll-a concentrations in the control (C) and N, P and N+P addition. Chlorophyll *a* concentration differences are mostly related to site variability (see control) rather than treatment (see Figure 27). Error bars are $\pm 1SD$.

These results suggest that there was a small positive response to the addition of N at all sites. This is despite there being more than 25 mg m^{-3} nitrate in the water column (Figure 15). Similarly, the small positive response to the addition of P at sites 1 and 3 was despite there being measurable DRP in the water column at that time (Figure 14). The positive response to the addition of N+P is consistent with the positive response for the addition of N. However, a slightly stronger response at sites 4 and 5, where chlorophyll *a* concentrations were highest (Figure 20), may indicate that the phytoplankton had run out of nutrients at those sites.

3.7 Zooplankton dilution experiment

The results of the zooplankton dilution experiment (Figure 29) show that at site 2 there was evidence of zooplankton grazing with the grazing rate at -0.257 per day almost balancing the growth at +0.280 per day ($r^2 = 0.744$, $n = 12$).

The results from site 5 show no growth as the chlorophyll *a* concentrations at the end of the incubation were all less than in the initial natural water. Given that site 5 had the highest chlorophyll *a* starting concentration and there was an indication of possible nutrient depletion at that site (Figure 29), the site 5 result is consistent with the incubation running out of nutrients.

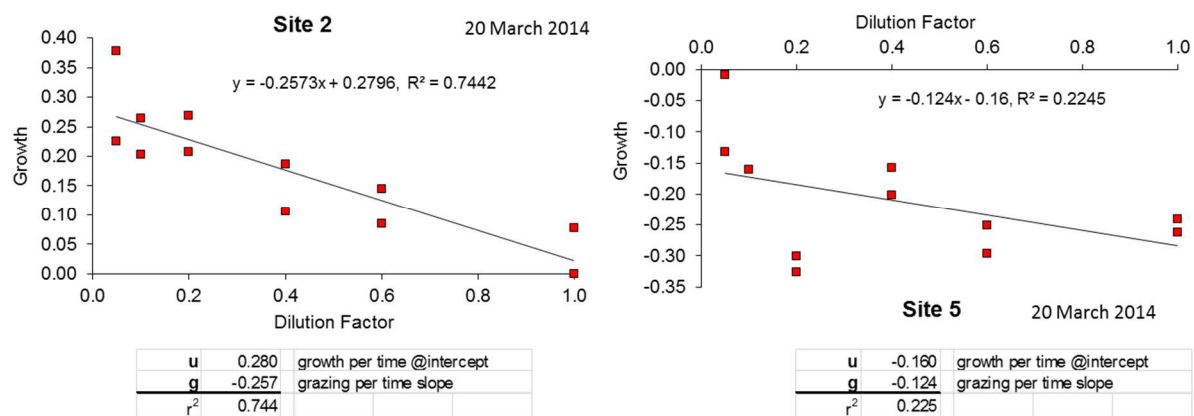


Figure 29: Plots of growth relative to dilution in the zooplankton dilution incubations at site 2 and 5 in March 2014. All data are plotted (see text for interpretation).

3.8 Acoustic Doppler Current Profiler (ADCP)

Acoustic Doppler current profiler was used on 13 March 2014 in bottom tracking mode on transects across the lake at sites 2, 3, 4, buoy, 5 and near the dam, to elucidate how water flows in the upper and lower water columns when the lake was thermally stratified.

The data were extracted from the ADCP files and converted into depth–distance plots of current velocity across the lake at each sampling point (Figure 30 to Figure 35). The plots include a vertical profile of current velocity and a profile of temperature and chlorophyll *a* concentration measured at the same time.

Because thermal stratification occurred at around 8 m depth, the mean velocity through a cross section 7.5 m deep in the upper water was compared with mean velocities through a similar cross section from 7.5 m to 15 m deep in the lower water column. The areas used for the cross sections are marked on the plots as white squares labelled A (upper) and B (lower).

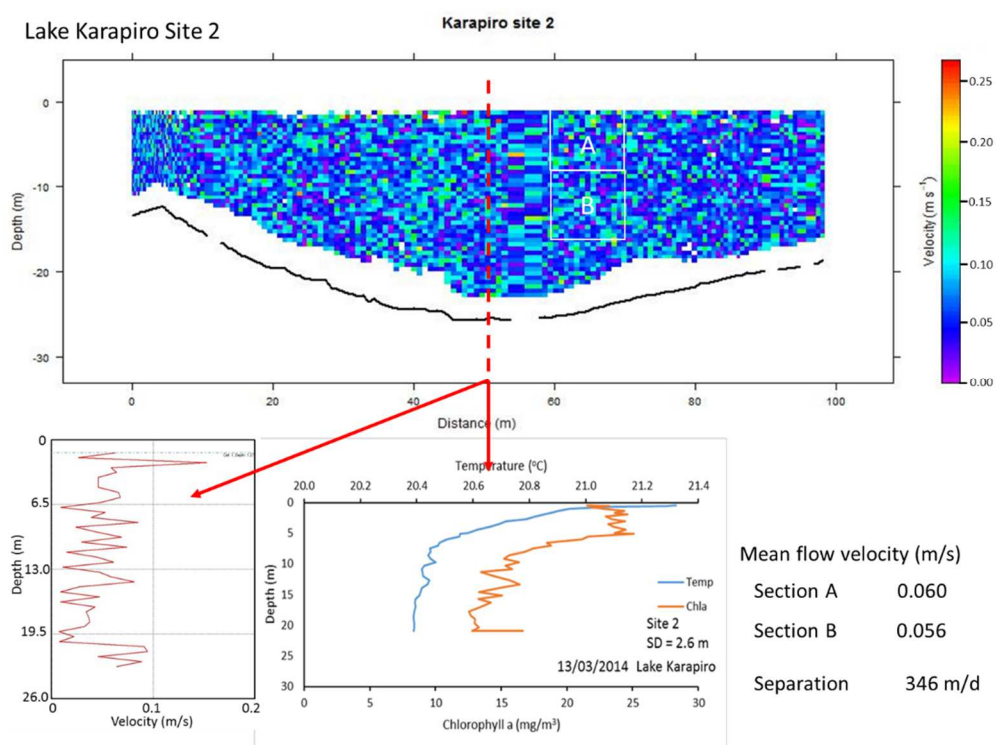


Figure 30: Depth-Distance current velocity profile contours at site 2. See text for full description.

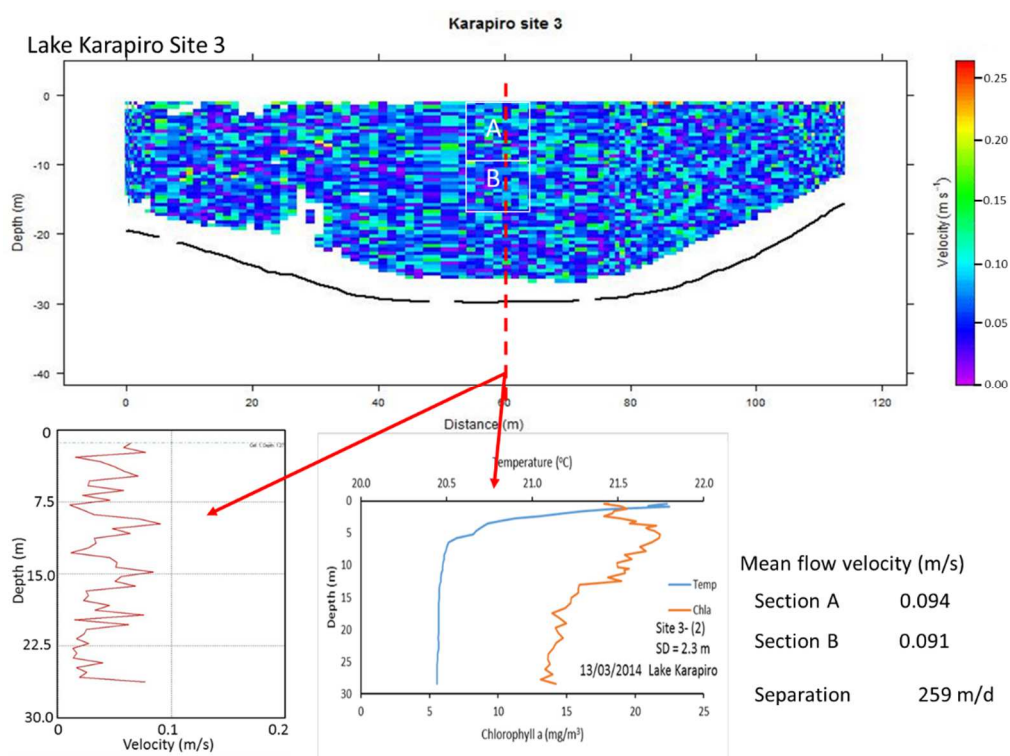


Figure 31: Depth-Distance current velocity profile contours at site 3. See text for full description.

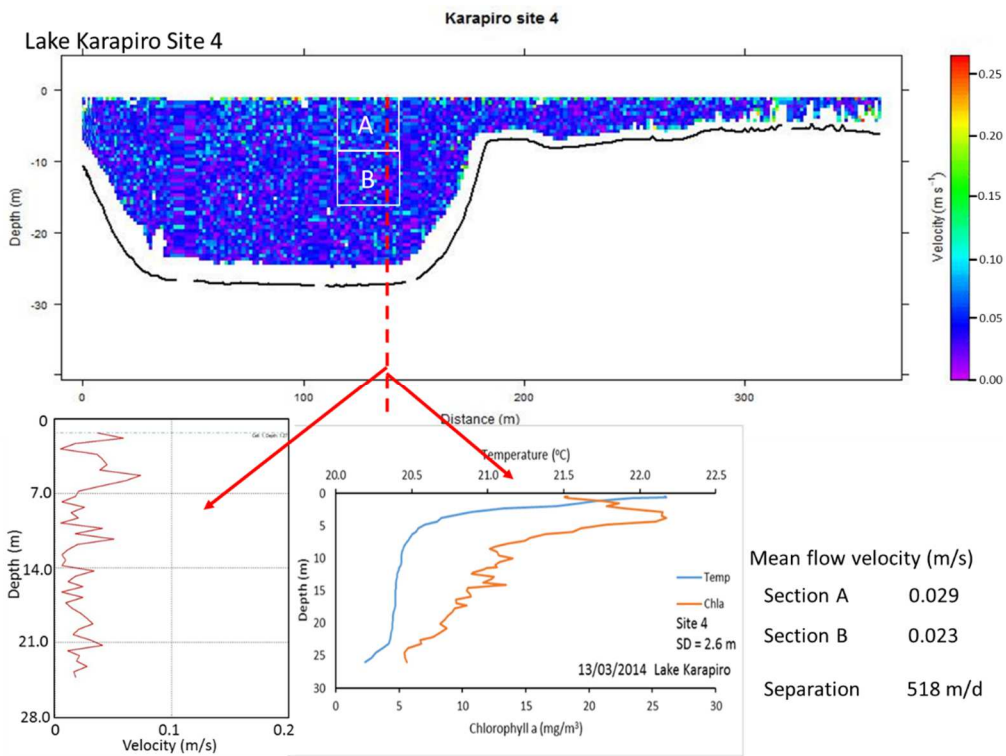


Figure 32: Depth-Distance current velocity profile contours at site 4 . See text for full description.

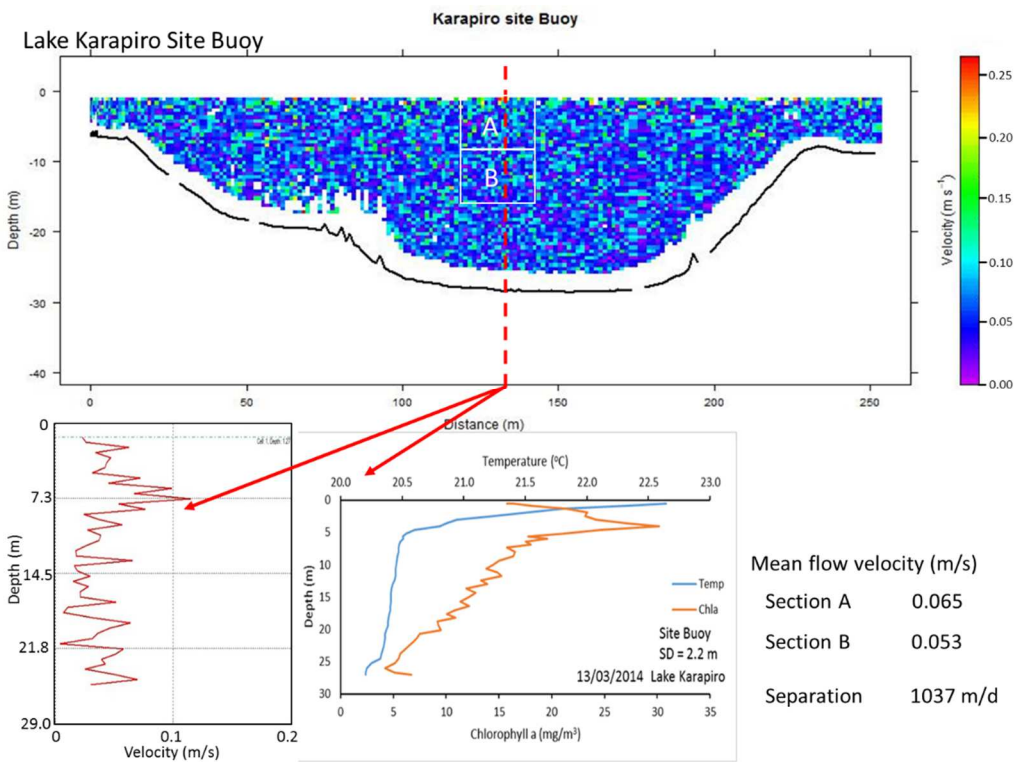


Figure 33: Depth-Distance current velocity profile contours at the Buoy site. See text for full description.

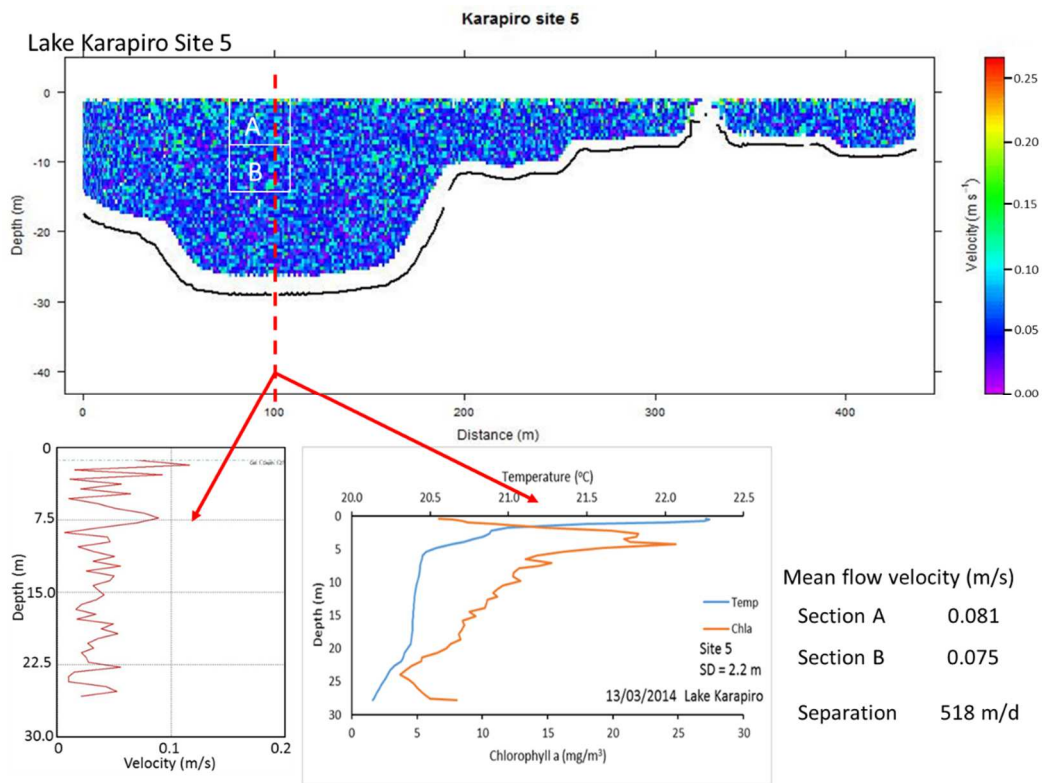


Figure 34: Depth-Distance current velocity profile contours at site 5. See text for full description.

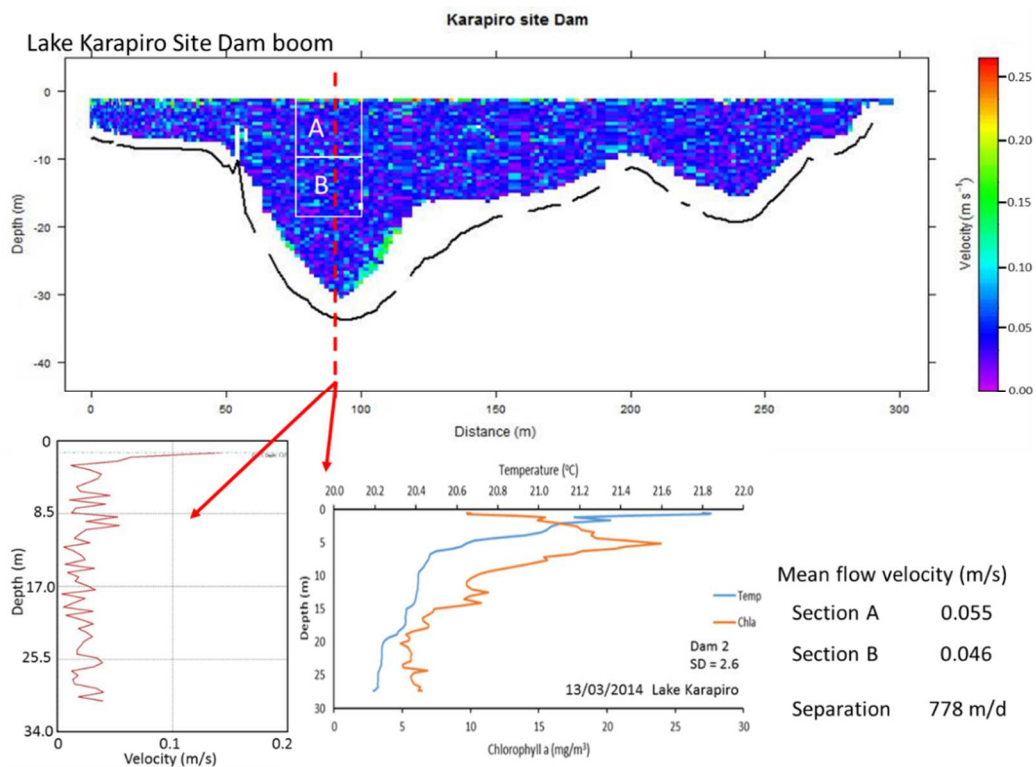


Figure 35: Depth-Distance current velocity profile contours near the dam. See text for full description.

In general, the mean current velocity through the middle of the lake on 13 March 2014 was around 0.065 m s^{-1} giving a mean residence time of about 4.5 days from site 1 to site 5. The assessment of upper and lower current velocities show small differences, which amount to large separations between upper and lower water columns over a day (Table 4).

Table 4: Mean current velocities (m/s) in the upper and lower water column at each site. The Upper - Lower is the velocity difference and the daily separation is an estimate of how far the upper water column would travel relative to the lower water column.

Site	Cross Section	Velocity (m/s)	Upper - lower (m/s)	Daily separation (m)
Site 2	Upper	0.060	0.004	345.6
	Lower	0.056		
Site 3	Upper	0.094	0.003	259.2
	Lower	0.091		
Site 4	Upper	0.029	0.006	518.4
	Lower	0.023		
Buoy site	Upper	0.065	0.012	1036.8
	Lower	0.053		
Site 5	Upper	0.081	0.006	518.4
	Lower	0.075		
Dam	Upper	0.055	0.009	777.6
	Lower	0.046		

Interpretation

Drawn as a schematic diagram (Figure 36, upper), it is apparent that these current velocity differences have effectively blocked vertical mixing forming a boundary between the upper and lower layers. This has confined some phytoplankton in the well-lit upper water column (euphotic zone) allowing their rapid growth, which has resulted in very large concentration gradients for chlorophyll across the boundary from site 2 downstream to the dam. However, at site 3, the chlorophyll concentrations were lower than at site 2 or site 4. Closer inspection of Figure 31 shows that the boundary was deeper at this site and extended to around 13 m depth, which is well below the euphotic zone (Figure 36, lower). Assuming the upper water column was fully mixed, this means that the phytoplankton at this site spent longer in the dark, which could reduce their growth due to light limitation. This effect is known as critical turbulence (Huisman et al. 1999) and is associated with critical depth³ (Sverdrup 1953).

Essentially, phytoplankton trapped below the boundary are below the critical depth and die, which is consistent with the reducing chlorophyll *a* concentrations below the boundary from site 2 downstream to the dam (Figure 36, upper).

³ The amount of time spent in the euphotic zone determines the rate at which phytoplankton biomass increases while the time spent in the dark determines the loss of phytoplankton biomass through cell death. The theoretical depth at which phytoplankton growth in the euphotic zone is matched by losses of phytoplankton biomass in the dark is known as the critical depth. Critical turbulence is the level of mixing that results in the phytoplankton reaching their critical depth

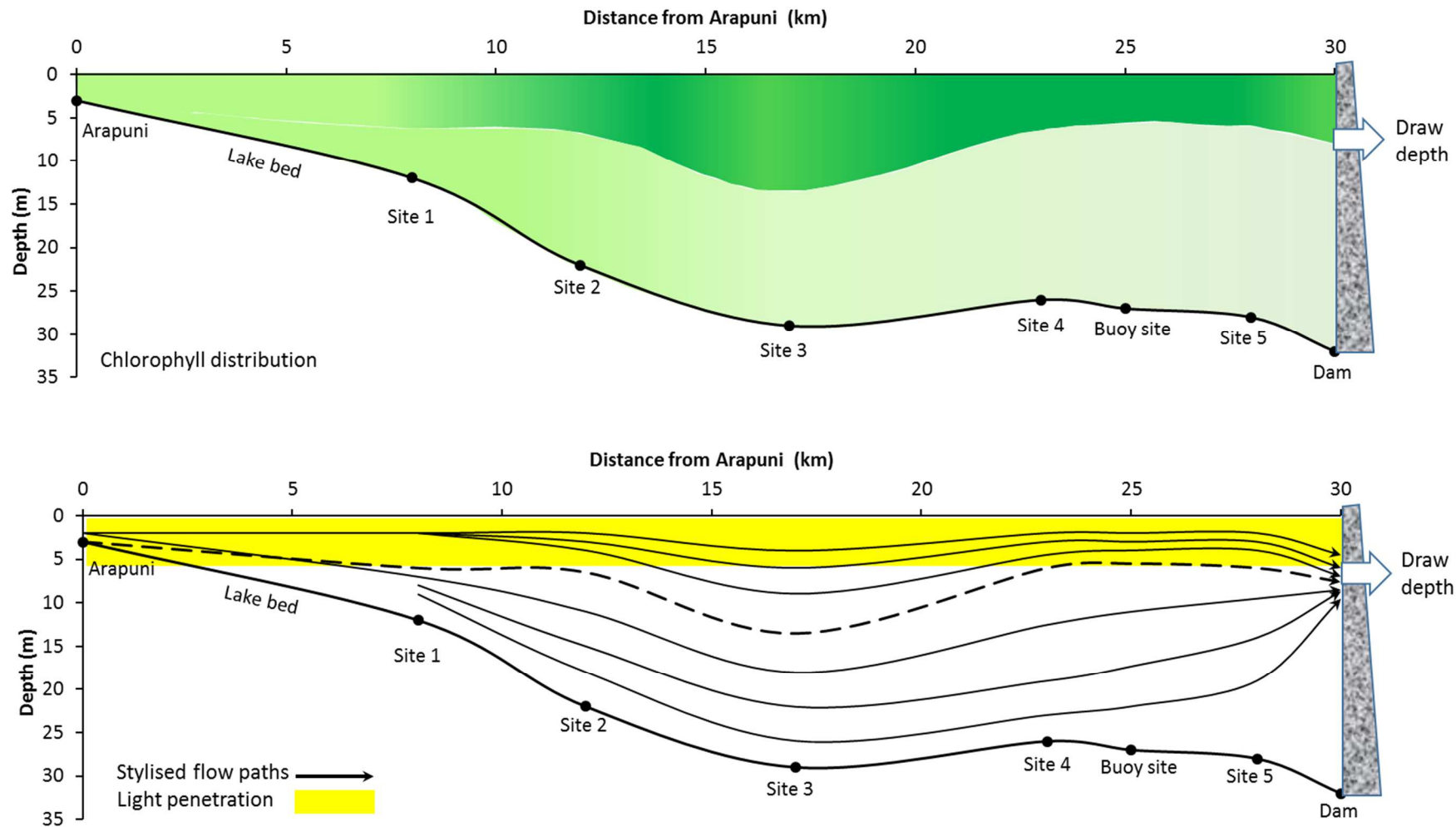


Figure 36: Longitudinal schematic diagrams of chlorophyll distribution (upper) and stylised flow paths (lower) in Lake Karapiro on 13 March 2014. Chlorophyll concentrations are indicated by the intensity of the green colour based on chlorophyll fluorescence data on 13-19 March 2014. The boundary between high and low chlorophyll concentrations (upper figure) is represented by the broken line (lower figure). Maximum light penetration (1% light level) was around 6 m at all sites (yellow block, lower figure). The stylised flow paths focus on the lake outlet to the Karapiro power station at about 8 m depth. Relative positions of sites are given below the lake bed. Vertical axis not to scale.

The current velocities at site 3 were around 30% higher than at site 2, which could mean that there is greater mixing at this site and the deepening of the boundary with lower chlorophyll concentrations may be partially due to dilution with the low chlorophyll concentration water from the lower water column.

Given that the 13 March 2014 data were measured during low flow conditions, at higher flows this mixing is likely to be stronger resulting in lower than expected chlorophyll *a* concentrations (Figure 18, Figure 19). Extended periods in low light may also explain why the net carbon uptake rates were very low at Site 3 in December 2013 and January 2014 (Figure 24), high and medium flow conditions respectively, but were comparable with all other sites in March and May 2014 when there were low flow conditions.

The effect observed at Site 3 was most likely due to changes in current velocity at that site rather than a change in retention time through the whole lake, because the net carbon uptake rates at the other sites were not affected in December 2013 and January 2013. This implies that, at the downstream sites, the phytoplankton had recovered from whatever caused their metabolic rate to reduce. One possible cause for reduced metabolic rates could be that, with very deep mixing (30 m) at site 3, the phytoplankton had exceeded their critical depth limit and were beginning to die.

The reduction in net carbon uptake rate effect was observed at a flow rate of just 35 m³ s⁻¹ higher than minimum low flow and was much stronger when the flow rate was 80 m³ s⁻¹ higher than minimum low flow (Figure 24, December 2013 and January 2014).

Chlorophyll *a* concentrations increased markedly in the upper water column of Lake Karapiro at sites 4 and 5, compared with sites 1 to 3, when there were low flow conditions and the lake was stratified in January and March 2014. Although there was some surface warming that might have initiated thermal stratification, the stratification observed was consistent with draw-induced stratification associated with the high level outflow from the lake to the power station (Spigel and Farrant 1984). The schematic diagram (Figure 36, lower figure) shows indicative flow paths in the upper and lower layers. The flow paths are shorter in the upper layer allowing the water above the boundary to move slightly faster than the water below the layer. This is consistent with the observed current velocities measured on 13 March 2014 (Table 4) where the upper layer was moving up to 0.012 m s⁻¹ faster. This flow difference allows the upper water to move up to a km per day further downstream than water in the lower layer (Table 4).

4 Discussion

Studies on the Waikato River and elsewhere show that the main factors that influence chlorophyll *a* concentrations include nutrient (either N or P) and light limitation, phytoplankton species (e.g., Magadza, 1978, 1979, 1980; Lam, 1979, 1981), retention time and thermal stratification (e.g., Coulter et al. 1983; Pridmore & McBride, 1984; Schallenburg & Burns, 1997; Bilinska, 2005). To have reducing chlorophyll *a* concentrations but increasing TN concentrations in the river over the last 10 years (Figure 1) would require P limitation or higher flow rates and thus shorter retention times.

Theoretically, higher flow rates will reduce the residence of water in Lake Karapiro thereby reducing the time available for phytoplankton growth and thus the uptake of $\text{NO}_3\text{-N}$ and DRP from the water column. If phytoplankton growth has a doubling time of ~ 0.5 days, the change in flow from a summer minimum flow of $\sim 153 \text{ m}^3 \text{ s}^{-1}$ to a high spring flow of $370 \text{ m}^3 \text{ s}^{-1}$ would have halved the potential phytoplankton growth and resulted in higher TN concentrations in the river water. However, once in the river, the phytoplankton will move with the water and can grow to the full potential of the dominant species limited only by the available nutrients and grazing pressure by zooplankton. Light penetrates to the river bed.

The results of this study are consistent with these theoretical expectations i.e., as flow reduced, phytoplankton biomass increased. However, the increase was not just a function of retention time, but included the effects of stratification, season and light limitation through exceedance of critical depth. Stratification was not simply a function of differential solar heating of the surface waters but included the effects of power station operation with draw-induced stratification being very important. In short, the factors affecting phytoplankton biomass in Lake Karapiro are complex and are summarised in more detail below.

Apart from growth, changes in chlorophyll concentrations may also be caused by allochthonous inputs or redistribution of chlorophyll biomass between different layers. To check for possible allochthonous inputs of chlorophyll, the chlorophyll concentrations at each site on each occasion were converted to aerial loads in the upper water column for a strip 1 m wide across the whole lake to a depth of 8 m (13 m at site 3) (Figure 37). Because the stratification isolates the upper layer from the lower layer (Figure 36), it is unlikely that chlorophyll produced below the depth of stratification would affect concentrations in the upper layer, although sedimentation of phytoplankton from the upper layer could reduce the overall biomass. The expectation from this transformation is that an allochthonous input of chlorophyll would be seen as a sudden change in the biomass between sites whereas growth would be seen as a gradual increase in biomass. This assumes that the integrated mean chlorophyll concentration is constant across the width of the lake.

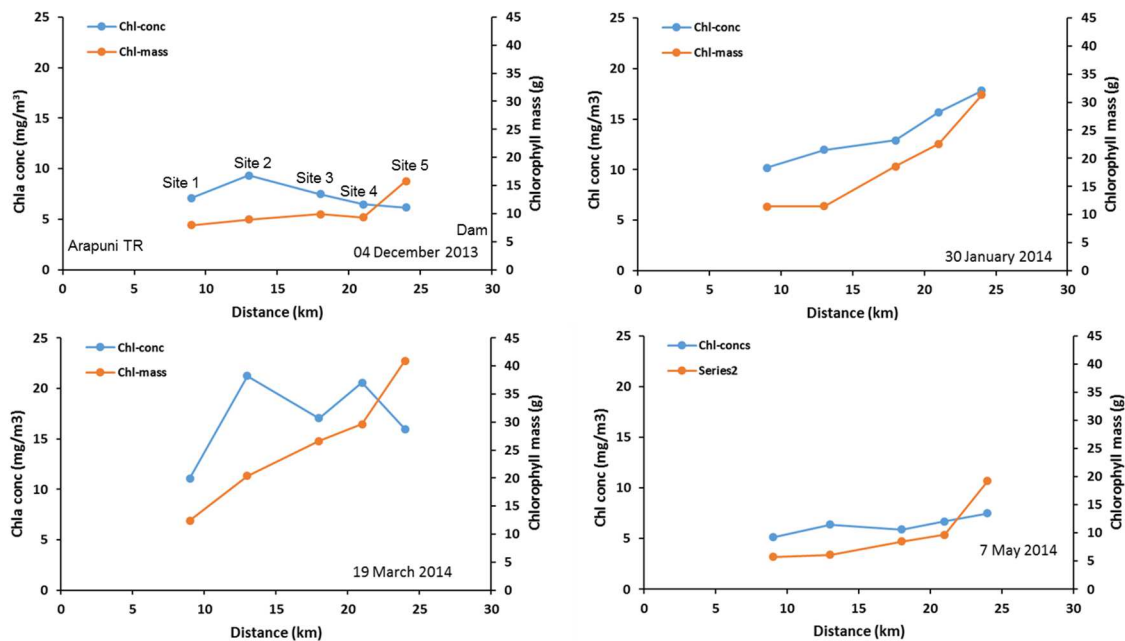


Figure 37: Changes in chlorophyll mass relative to concentration at the 5 sites on each of 4 occasions. Mass calculated for a 1 m wide strip 8 m deep across the width of the lake at each site using integrated mean chlorophyll concentrations from the CTD-Fluorescence profiles (Figure 18 to 21) and estimated width data (Table 1).

Within the limitations and potential errors of these transformations, it is unlikely that there is a substantial allochthonous chlorophyll biomass input between sites 1 and 2 in the upper part of the lake. However, the sudden increase in chlorophyll biomass at site 5 suggests that there may be an allochthonous input near site 5. Observations at the time of sampling noted that westerly winds can cause the surface waters of the lake to move upstream. This effect could transport chlorophyll biomass from the large embayment adjacent to the dam to site 5 or further upstream. Other sources of chlorophyll biomass could include lateral dispersion of epiphytes dislodged from the macrophyte leaves by boat wakes and wind-waves. No measurements were made to assess this potential source.

While the zooplankton grazing experiment suggests that zooplankton grazing pressure may be able to balance phytoplankton growth (Figure 29), the correlation between dominant phytoplankton species and dominant zooplankton species in December 2013 (Table 2) may indicate that zooplankton grazing could be influencing the phytoplankton species composition. Cladocera are unlikely to be able to consume large diatoms and consequently these may become dominant due to selective grazing of smaller, more easily consumed species.

4.1 Summary

4.1.1 Lake water column structure

In summer, the water quality in Lake Karapiro undergoes a change from the source water leaving the Arapuni hydro lake to the outflow from the Karapiro dam. Although TN and TP concentrations were essentially the same in the upper and lower water column at all sites, the DRP and NO₃-N concentrations were lower in the upper 5 m of the water column than at 1-2 m above the bottom from site 2 downstream to the dam in January and March 2014. Whereas the TN and TP data imply vertical mixing, the DRP, NO₃-N and NH₄-N data imply stratification. This difference in the DRP and NO₃-N data was caused by phytoplankton growth in the upper water column. That the TN and TP

data were essentially the same in the upper and lower water column implies almost stoichiometric conversion of the DRP and NO₃-N into chlorophyll and thereby phytoplankton biomass.

Vertical profiles of depth-referenced temperature, DO, light and chlorophyll fluorescence, together with thermistor / DO chain data confirmed that stratification occurred in Lake Karapiro in summer. The chlorophyll fluorescence data also confirmed the increase in chlorophyll concentrations in the near surface waters showing that the high phytoplankton biomass was confined to the upper 8 m with a very sharp gradient to low biomass below this boundary. The 1% light level was around 6-7m at this depth.

Anoxia of a thin layer of bottom water was indicated during periods of stratification during the summer period. Concentrations of DRP and NH₄ in the bottom waters of the lake increased with increasing distance downstream, suggesting that in-lake processes do contribute to internal nutrient recycling. Rapid mixing of nutrients released from anoxic sediments under oxic water column conditions can therefore not be ruled out. Mineralisation processes in the water column are also likely to be important for internal nutrient recycling, particularly at downstream locations where hypolimnion depths exceed 20 m.

It is unclear why surface inorganic nutrient concentrations increased with increasing distance downstream during early summer (December), when flow rate and water retention time was high and chlorophyll-a concentrations were low and decreasing downstream. Nutrient concentrations in the Lake Arapuni inflow were lower than surface and bottom measurements across all sites and there are no major downstream tributaries below the Pokaiwhenua inflow.

It is suggested that the mobilisation and decay of hornwort (*Ceratophyllum demersum*) plants under high flow conditions may have contributed to the observed nutrient increase. The extensive macrophyte beds present in the lake together with frequent detachment and transport of plant material downstream as a result of changing flow patterns are likely to have significant impacts on internal nutrient cycling and availability.

4.1.2 PPR experiments

The ¹⁴C-carbon PPR experiments show that, on each occasion, the net carbon uptake rates (i.e., phytoplankton growth rates) in the upper 5 m of water column were almost the same at all sites. This is consistent with the almost stoichiometric conversion of nutrients into phytoplankton biomass. There were large differences in net carbon uptake rates between sampling occasions in summer with the lowest uptake rates in December 2013 (highest flow) and the highest uptake rates in January and March 2014 (medium and low flow, respectively). This implies that chlorophyll *a* concentrations are likely to be a function of residence time in the lake in summer, and will increase to the limit of the available nutrients in the upper water column, as the discharge from the Karapiro dam reduces. In autumn (May 2014) despite low flows, the net carbon uptake rates were substantially lower (~5%) than in March 2014, indicating that light limitation was an important consideration at that time.

4.1.3 Nutrient bioassay experiment

A set of nutrient addition bioassays in March (low flow, stratified) indicated that phytoplankton biomass increased by 20-30% per day at all sites with the addition of N and increased by up to 20% per day at sites 1 and 3 only with the addition of P. The addition of N+P resulted in a 20% per day increase in biomass at sites 1 to 3 and a 35-40% per day increase in biomass at sites 4 and 5. These results indicate that there was possible N-limitation of phytoplankton growth in Lake Karapiro in March 2014. The larger response to the N+P addition at sites 4 and 5, where the highest chlorophyll

a concentrations were recorded may indicate that the phytoplankton had almost run out of nutrients. This is consistent with the low DRP and NO₃-N concentrations in the upper water column at that time. The timing of the experiment coincided with a period of thermal stratification when water flows were low, lake residence times were long and critical mixing depth, and therefore light limitation, was reduced.

A greater response to addition of both N and P compared with the response to adding just N or P (co-limitation) is not uncommon and has been found in many nutrient bioassays (e.g., Müller & Mitrovic, 2015). This implies that input of N as well as of P should be considered in the management of phytoplankton growth.

4.1.4 Zooplankton bioassay experiment

A zooplankton dilution bioassay in March at sites 2 and 5 showed that phytoplankton growth was slightly greater than zooplankton grazing pressure at site 2 and that the incubations had run out of nutrients at site 5, consistent with the results from the nutrient addition incubations. Zooplankton grazing is therefore suggested to impact phytoplankton production at upstream locations while at downstream locations, nutrient availability is likely to exert a greater influence on phytoplankton biomass when surface chlorophyll-*a* concentrations are high. As the experiments coincided with relatively low zooplankton biomass and a period of rotifer and copepods dominance, the impact of grazing is likely to be higher in other periods when Cladocera were dominant. It is unclear why a large structural shift in zooplankton community composition from Cladocera to copepod and rotifer dominance occurred between early and mid-summer. A suggestion is that they may have run out of appropriate size phytoplankton species to consume as the large diatom species became dominant.

4.1.5 The influence of flow, morphometry and stratification

Current measurements under low flow stratified conditions in March 2014 found that the mean flow through the lake was around 0.065 m s⁻¹ giving a theoretical mean residence time from site 1 to the dam of around 4.5 days. The current measurements also showed that mean current velocities were slightly higher in the upper than lower water column. This small difference (up to 0.012 m s⁻¹) was sufficient to allow the upper water column to move as much as a km per day further downstream than the lower water column separated by the boundary.

While net carbon uptake rates were nearly the same at all sites on each occasion, there were some differences between the upstream site (site 1) and downstream site (site 5) in December 2013 with the site 5 net carbon uptake rates about 40% lower. In May the pattern was reversed. There were also two other notable exceptions at site 3 in December 2013 and January 2014 when the site 3 net carbon uptake rates were substantially lower (~5%) than at sites 2 and 4 immediately upstream and downstream. These site 3 anomalies imply that the low PPR values were an artefact of the site rather than a retention time effect.

Current measurements at site 3 on 13 March 2014 found current velocities were up to 30% higher than at the other sites, and the profile data showed that the boundary between upper and lower layers was twice as deep. This suggests that the channel morphometry at site 3 was affecting the hydrodynamics causing turbulence and that phytoplankton were mixed deeper into the water column, thereby spending longer in the dark at site 3 than at the other sites (Huisman et al. 1999). There was no indication that dilution played a part as there was essentially no difference in the upper water column chlorophyll *a* concentrations between Sites 1, 2 and 3 in December 2013 and January 2014 (Figure 17) and thereby no biomass difference to account for the substantially lower carbon

uptake rates at Site 3 on those two occasions. This indicates that the phytoplankton were experiencing light limitation at site 3 and were not capable of rapid growth. The travel time to site 4 downstream was in the order of a day which appears to have been sufficient to allow them to recover.

Current velocity at the other sites in December 2013 may also have been causing a similar effect. The maximum water column depth at site 1 was around 10 m and the water reaching that site had been less than 5 m deep for many hours so that light limitation was unlikely. However, by the time the water reached site 5 near the dam, the water depth was around 30 m and vertical mixing (Figure 18) could have caused some level of light limitation.

These results indicate that retention time, stratification, deep mixing and light limitation, are all important factors affecting chlorophyll *a* concentrations in the hydro lakes on the Waikato River in summer. Consequently, the processes occurring in the hydro lakes are likely to be major factors influencing chlorophyll *a* concentrations in the Waikato River.

The issue at the focus of this study was why have there been trends of increasing mean TN but decreasing mean chlorophyll *a* concentrations in the Waikato River over the last 20 years, when the expectation would be for chlorophyll *a* concentrations to increase in concert with TN.

Retention time affects both chlorophyll *a* and nitrate concentrations in a stoichiometric inverse relationship, as found in this study. This means that, with higher flows and shorter residence/retention times in the hydro lakes, phytoplankton can't grow as much and not as much nitrate is taken up. The stoichiometric relationship means that the chlorophyll concentrations will decrease and the nitrate concentrations will increase proportionally. No N is gained so the TN concentrations should not rise. This implies that there is another factor that has not been considered.

The nitrate trend data presented by Vant (2013) has a cyclical pattern with high concentrations in winter and low concentrations in summer (Figure 1). As nitrate is mostly derived from groundwater leaching, and concentrations would decrease due to dilution in wet weather, the expectation would be for nitrate concentrations in the Waikato River to be relatively constant and decrease in winter. However, N concentrations and thus loads are higher in winter, which suggests that there is a high N background being reduced by plant uptake.

Consequently, it is almost certain that the cyclical pattern in N (Figure 1) is caused by plant uptake in summer. This means by phytoplankton, but also includes the aquatic macrophytes, which also take nutrients from the water. If nutrient assimilation by aquatic macrophytes is reduced as flows increase, then TN concentrations could increase. The effect of aquatic macrophytes on nutrient supply may require further investigation.

This report has not considered the possible effect of any phytoplankton growth that might occur in winter in the hydro lakes. Lake Taupo has a winter bloom.

4.2 Conclusions

Phytoplankton dynamics

1. The seasonal growth of phytoplankton occurs mostly from January to March, when water discharges are lowest and residence time highest.

2. Surface chlorophyll-a concentration generally increased with distance from Lake Arapuni, with the largest increases coinciding with higher water temperatures, thermal stratification (January) and increased water residence times associated with lower flow rates though the Karapiro dam.
3. Water column stratification reduces the depth of the surface mixed layer, leading to reduced light limitation during periods of increased water retention.
4. The presence and depth of the surface mixed layer is primarily regulated by draw-induced stratification associated with the high level outflow to the power station. The impact of thermal stratification due to the cold water inflow from Lake Arapuni (early summer) or solar warming of the surface waters (mid-summer) is suggested to be minor in comparison.
5. Channel morphology has a strong influence on the critical mixing depth, particularly in the mid-reaches of the lake (Site 3) where a deeper mixing depth reduces phytoplankton productivity during periods of medium and high flow because of reduced average PAR over the mixed depth.
6. Nutrient limitation may become important during periods of thermal stratification, low-flow and long lake residence times, when the critical mixing depth and therefore light limitation is reduced, growth rates are higher and nutrient depletion in the surface waters occurs, particularly at downstream locations.
7. Nutrient availability is likely to exert a greater influence on phytoplankton biomass than grazing at downstream sites, when surface chlorophyll-a concentrations are high.
8. Zooplankton grazing is suggested to impact phytoplankton production at upstream locations during periods when assimilable phytoplankton species are abundant, as observed through the zooplankton dilution experiments conducted at two sites in March.
9. It is unclear why a large structural shift in zooplankton community composition from cladocera to copepod and rotifer dominance occurred between early and mid-summer.

Lake nutrient cycling

1. Increasing concentrations of DRP and $\text{NH}_4\text{-N}$ in the bottom waters of the lake with increasing distance downstream suggest that in-lake processes do contribute to internal nutrient recycling. The release of nutrients from anoxic sediments under oxic water column conditions can therefore not be ruled out.
2. The impact of macrophyte (hornwort, *Ceratophyllum demersum*) and associated epiphyte biomass on nutrient assimilation, recycling and availability to phytoplankton is currently unclear but is likely to be significant given the extensive macrophyte beds present in the lake.
3. Nutrient attenuation by littoral macrophyte beds is thought to be especially important during stratified and low-flow conditions, when shallow groundwater is likely to represent the principal source of nutrients to the surface waters of the lake. Shallow groundwater enters at the depth of the macrophyte weed beds and nutrients must pass through the littoral weed beds to reach the open waters of the lake.
4. A reduction in macrophyte biomass and assimilative capacity may therefore lead to a potential increase in nutrient availability to phytoplankton.

Impact of increasing nutrient loads on Lake Karapiro phytoplankton biomass

1. Increases in nutrient availability over the summer growth period may lead to increases in phytoplankton biomass but only under stratified and low-flow conditions.
2. Increases in nutrient availability outside of the summer growth period are not likely to impact phytoplankton biomass.
3. The phytoplankton response to additional nutrients, as measured in March, is likely to be greater for increasing nitrogen or nitrogen and phosphorus together than for phosphorus alone.

5 Acknowledgements

Gareth Van Assema for collecting the upstream samples, George Payne for collecting the ambient PAR light data, Christine Roper, and Greg Olsen for occasional assistance in sampling and sample processing on the boat, Scott Edhouse, David Bremner, Aleki Taumoepeau and Sam Parks for driving the boats as required, Rowing New Zealand for recovering the thermistor chain prior to the weed boom removal and Mighty River Power Ltd for providing lake flow and water level data.

6 References

- Bilinska, K. (2005) *Thermal Stratification in the Waikato hydro lakes*. Thesis for BE (Environmental), University of Western Australia.
- Coulter, G.W., Davies, J., Pickmere, S. (1983) Seasonal and limnological change and phytoplankton production in Ohakuri, a hydro-electric lake on the Waikato River. *New Zealand Journal of Marine and Freshwater Research*, 17: 169-183.
- Gallegos, C.L., Vant, W.N., Safi, K.A. (1996) Microzooplankton grazing of phytoplankton in Manukau Harbour, New Zealand. *New Zealand Journal of Marine and Freshwater Research*, 30: 423-434.
- Huisman, J., Oostveen, P. van, Weissing, F. J. (1999) Critical depth and critical turbulence: two different mechanisms for the development of phytoplankton blooms. *Limnology and Oceanography*, 44(7): 1781-1787.
- Lam, C.W. (1979) Dynamics of phytoplankton growth in the Waikato River, North Island, New Zealand. *Hydrobiologia*, 66: 237-244.
- Lam, C.W. (1981) Ecological studies of phytoplankton in the Waikato River and its catchment. *New Zealand Journal of Marine and Freshwater Research*, 15: 95-103.
- Lauridsen, T.L., Søndergaard, M., Jensen, J.P., Jeppesen, E. (red.) (2005) Undersøgelser i søer. NOVANA . *Danmarks Miljøundersøgelser. - Teknisk anvisning fra DMU* 22: 233.
- Magadza, C.H.D. (1978) Phytoplankton in six hydroelectric lakes on the Waikato River, New Zealand, 1970–72. *New Zealand Journal of Marine and Freshwater Research*, 12: 29-40.
- Magadza, C.H.D. (1979) Physical and chemical limnology of six hydroelectric lakes on the Waikato River, 1970–72. *New Zealand Journal of Marine and Freshwater Research*, 13: 561-572.
- Magadza, C.H.D. (1980) Comparative seasonal estimates of primary productivity in the Waikato River lakes during summer, autumn, and winter. *New Zealand Journal of Marine and Freshwater Research*, 14: 71-77.
- Müller, S., Mitrovic, S.M. (2015) Phytoplankton co-limitation by nitrogen and phosphorus in a shallow reservoir: progressing from the phosphorus limitation paradigm. *Hydrobiologia*, 744: 255-269.
- Pridmore, R.D., McBride, G.B. (1984) Prediction of Chlorophyll a concentrations in impoundments of short hydraulic residence time. *Journal of Environmental Management*, 19: 343-350.
- Rutherford, J.C., Williamson, R.B., Davies-Colley, R.J., Shankar, U. (2001) Waikato Catchment Water Quality Model. *NIWA client report* number ELE90229/3 to Mighty River Power Ltd. 124 pp.
- Schallenburg, M., Burns, C.W. (1997) Phytoplankton biomass and productivity in two oligotrophic lakes of short hydraulic residence time. *New Zealand Journal of Marine and Freshwater Research*, 31: 119-134.

- Spigel, R.H., Farrant, B. (1984) Selective withdrawal through a point sink and pycnocline formation in a linearly stratified fluid. *Journal of Hydraulic Research*, 22: 35-51.
- Steeman-Nielsen, E. (1952) The use of radioactive carbon (C14) for measuring organic production in the sea. *J. Cons. Int. Explor. Mer.* 18: 117-140. [Full journal name: *Journal du Conseil / Conseil Permanent International pour l'Exploration de la Mer*].
- Sverdrup, H.U. (1953) On conditions for the vernal blooming of phytoplankton. *Journal du Conseil International pour l'Exploration de la Mer*, 18: 287-295.
- Vant, W.N. (2013) Trends in river water quality in the Waikato region, 1993-2012. *Waikato Regional Council Technical Report 2013/20*.
- White, E., Payne, G.W. (1977) Chlorophyll production, in response to nutrient additions, by the algae in Lake Taupo water. *New Zealand Journal of Marine and Freshwater Research*, 11: 501-507.
- Yu Y., Zhang W., Xiao T., Li H., Li C., Sun S. (2010) Impact of microzooplankton and *Calanus sinicus* (Brodsky, 1962) on phytoplankton in the Yellow Sea during early summer. *Chinese Journal of Oceanology and Limnology*, 28(4): 881-886. DOI: 10.1007/s00343-010-9916-0

Appendix B Zooplankton

Zooplankton species by date and site

Site date	Site 1 4-Dec-13	Site 2 4-Dec-13	Site 3 4-Dec-13	Site 4 4-Dec-13	Site 5 4-Dec-13	Site 1 30-Jan-14	Site 2 30-Jan-14	Site 3 30-Jan-14	Site 4 30-Jan-14	Site 5 30-Jan-14	Site 1 19-Mar-14	Site 2 19-Mar-14	Site 3 19-Mar-14	Site 4 19-Mar-14	Site 5 19-Mar-14	Site 1 7-May-14	Site 2 7-May-14	Site 3 7-May-14	Site 4 7-May-14	Site 5 7-May-14	
biomass (ug/L)																					
Copepods																					
Acanthocyclops robustus	0.307	0.922	0.553	0.184	0.184	0.678	0.848	0.848	0.848	0.848	0.583	0.728	0.291	0.146	0.146	0	0	0	0	0.337	
Attheyella maorica	0	0	0	0	0	0	0	0	0	0	0	0	0	0	0	0	0	0	0	0	
Calanocia lucasi	0	0	0	0	0	0	0	0	0	0	0	0	0	0	0	0	0	0	0	0	
Copepod nauplii	0	0.100	0.400	0.900	0.400	0.200	3.500	1.000	3.500	6.500	0.875	2.175	1.350	0.150	0.150	0.100	0.563	0.600	0.200	1.500	
Cladocerans																					
Alona sp.	0	0	0.229	0	0.131	0	0	0	0	0	0	0	0	0	0	0.141	0	0.108	0	0	
Bosmina meridionalis	15.378	20.934	15.775	5.159	2.083	0.842	1.404	3.744	2.340	0.468	0.278	0	0.076	0	0	0	0	0	0	0	
Chydorus sp.	0	0.520	0	0.347	0.173	0	0	0	0.911	0	0.142	0.071	0	0	0	0	0	0.142	0	0	
Daphnia galeata	22.336	16.082	1.191	0	0	0	0	0	0	0	0	0	0	0	0	0	0	0	0	0	
Ilyocryptus sordidus	0	0	0	0	0	0	0	0	0	0	0	0	0	0	0	0	0	0	0	0	
Rotifers																					
Ascomorphella volvocicola	0.040	0.090	0.054	0.022	0.046	0	0	0	0	0	0	0	0	0	0	0	0	0	0	0.023	
Asplanchna brightwelli	0	0	0	0	0	0	0	0	0	0	0	0	0	0	0	0	0	0	0	0	
Asplanchna priodonta	0.475	1.140	0.570	0.684	0	0.114	1.710	7.410	0	0	0	0.684	0.171	0	0.086	0	0	0	0	0.428	
Bdelloids	0.010	0.008	0.008	0.016	0.008	0.040	0.020	0	0.060	0.140	0.015	0.015	0.060	0.006	0	0.006	0.008	0.006	0.004	0.030	
Brachionus angularis	0	0	0	0	0	0	0	0	0	0	0	0	0	0	0	0	0	0	0	0	
Brachionus budapestinensis	0	0	0	0	0	0	0	0	0	0	0	0	0	0	0	0	0	0	0	0	
Brachionus calyciflorus	0	0	0	0	0	0	0	0	0	0	0.000	0.122	0.081	0.081	0.041	0	0	0	0	0	
Brachionus quadridentatus	0	0	0	0	0	0	0	0	0	0	0	0	0	0	0	0	0	0	0	0	
Cephalodella gibba	0	0	0	0	0	0	0	0	0	0	0	0	0	0	0	0	0	0	0	0	
Collotheca sp.	0.004	0.002	0.015	0.025	0.003	0.017	0.101	0.101	0.050	0.050	0.020	0.044	0.033	0.039	0.010	0.002	0.003	0.003	0	0	
Conochilus dossuarius	0	0	0	0	0	0	0	0	0	0	0	0	0	0	0	0	0	0	0	0	
Conochilus unicornis	0	0	0	0	0	0	0	0	0	0	0	0	0	0	0	0	0	0	0	0	
Dicranophorus sp.	0	0	0	0	0	0	0	0	0	0	0	0	0	0	0	0	0	0	0	0	
Epiphanes macrourus	0	0	0	0	0	0	0	0	0	0	0	0	0	0	0	0	0	0	0	0	
Euchlanis deflexa	0	0	0	0	0.008	0	0	0	0	0	0	0	0	0	0	0	0	0	0	0	
Euchlanis dilatata	0	0	0	0	0	0	0	0	0	0	0	0	0	0	0	0	0	0	0	0	
Euchlanis meneta	0	0	0	0	0	0.008	0.080	0.040	0.040	0.120	0.042	0.012	0.012	0.024	0.006	0.004	0	0	0	0	
Filinia novaezealandiae	0	0	0	0	0	0	0	0	0	0	0	0	0	0	0	0	0	0	0	0	
Gastropus hyptopus	0	0	0	0	0	0	0	0	0	0	0	0	0	0	0	0	0	0	0	0	
Hexarthra intermedia	0	0	0	0	0	0	0	0	0.058	0.406	0	0	0	0	0	0	0	0	0.023	0	
Keratella cochlearis	0.005	0.008	0.005	0.015	0.005	0.046	0.319	0.217	0.662	0.413	0.002	0.014	0.033	0.021	0.002	0.013	0.026	0.037	0.034	0.092	
Keratella procurva	0	0	0	0	0	0	0	0	0	0	0	0	0	0	0	0	0	0	0	0	
Keratella slacki	0	0	0	0	0	0	0	0	0	0	0	0	0	0	0	0	0	0	0	0	
Keratella tecta	0	0	0	0	0	0	0.038	0.023	0.032	0.015	0.001	0.002	0.001	0.001	0	0.013	0.042	0.081	0.025	0.147	
Keratella tropica	0	0	0	0	0	0	0	0	0	0	0	0	0	0	0	0	0	0	0	0	
Lecane bulla	0	0	0	0	0	0	0	0	0	0	0	0	0	0	0	0	0	0	0	0	
Lecane closteroerca	0	0	0	0	0	0	0	0	0	0	0	0	0	0	0	0	0	0	0	0	
Lecane flexilis	0	0	0	0	0	0	0	0	0	0	0	0	0	0	0	0	0	0	0	0	
Lecane luna	0	0	0	0	0	0	0	0	0	0	0	0	0	0	0	0	0	0	0	0	
Lecane lunaris	0	0	0	0	0	0	0	0	0	0	0	0	0	0	0	0	0	0	0	0	
Lepadella accuminata	0	0	0	0	0	0	0	0	0	0	0	0	0	0	0	0	0	0	0	0	
Monommata sp.	0	0	0	0	0	0	0	0	0	0	0	0	0	0	0	0	0	0	0	0	
Mytilina ventralis	0	0	0	0	0	0	0	0	0	0	0	0	0	0	0	0	0	0	0	0	
Polyarthra dolichoptera	0.068	0.133	0.224	0.428	0.153	1.306	4.335	11.220	8.721	9.333	0.349	3.205	2.785	3.932	4.842	0.326	2.869	0.383	0.643	11.666	
Pompholyx complanata	0	0	0	0	0	0	0	0	0	0	0	0	0	0	0	0	0	0	0	0	
Squatina mutica	0	0	0	0	0	0	0	0	0	0	0	0	0	0	0	0	0	0.001	0	0	
Synchaeta oblonga	0.017	0.020	0.030	0.270	0.630	0.390	2.500	2.200	1.600	2.000	0.030	0.030	0.068	0.023	0.030	0.460	1.519	1.350	0.850	8.775	
Synchaeta pectinata	0	0	0	0	0	0	0	0	0	0	0	0	0	0	0	0	0	0	0	0	
Trichocerca porcellus	0.011	0.005	0.005	0.005	0	0.009	0	0.023	0	0	0	0	0	0	0	0	0	0	0	0	
Trichocerca pusilla	0.021	0.119	0.139	0.274	0.225	0	0	0	0	0	0	0	0	0	0	0.009	0.047	0.029	0	0.011	
Trichocerca similis	0.057	0.069	0.241	0.442	0.207	0.356	1.435	2.926	2.467	2.381	0.106	0.207	0.207	0.133	0.349	0.043	0.258	0.138	0.184	1.506	
Trichocerca stylata	0	0	0	0	0	0.006	0.040	0.010	0.010	0.040	0.007	0.014	0.003	0.003	0.002	0.001	0.004	0	0.014	0.023	
Trichocerca tenuior	0	0	0	0	0	0	0	0	0	0	0	0	0	0	0	0	0	0	0	0	
Trichotria tetractis	0	0	0.005	0	0.005	0	0	0	0	0	0.001	0.003	0.000	0.017	0.003	0	0	0.007	0.000	0	
Total																					
Copepods	0.307	1.022	0.953	1.084	0.584	0.878	4.348	1.848	4.348	7.348	1.458	2.903	1.641	0.296	0.296	0.100	0.563	0.600	0.200	1.837	
Cladocerans	37.714	37.536	17.195	5.506	2.388	0.842	1.404	3.744	3.251	0.468	0.420	0.071	0.076	0	0	0.141	0	0.251	0	0	
Rotifers	0.716	1.593	1.295	2.185	1.290	2.297	10.576	24.169	13.700	14.899	0.607	4.351	3.452	4.286	5.370	0.878	4.775	2.034	1.777	22.700	

Appendix C Sediment traps

Data from the sediment traps was effectively rendered unusable because of drifting weed (Hornwort) tangling with the traps. Consequently, there was no certainty that the sediment caught had fallen from the water column or was from the weed mass around the trap.

Of the data that appeared less affected by weed (19 March 2014), the sedimentation rate was about $100 \text{ g m}^{-2} \text{ d}^{-1}$ at site 5 and comprised about $200 \mu\text{g g}^{-1}$ chlorophyll *a* and $240 \mu\text{g g}^{-1}$ phaeophyton. The high proportion of chlorophyll and phaeophyton indicates that the source of this material was most likely phytoplankton. However, it is not certain whether the phytoplankton were pelagic (water column) or resuspended benthic (growing on the sediment) species. Given the depth of water (27 m) at site 5, light limitation should have prevented benthic material growing.

However, on standing in the light, the phytoplankton appeared to form a mat on the surface of the sediment (Figure C1) reminiscent of a cyanobacteria mat. This may imply that the organic matter (phytoplankton) had been washed off the leaves of the hornwort. While this outcome has little value for the present study, it does indicate that the huge biomass of macrophytes in Lake Karapiro is likely to be having a substantial effect of the nutrient load in the lake and the downstream river.

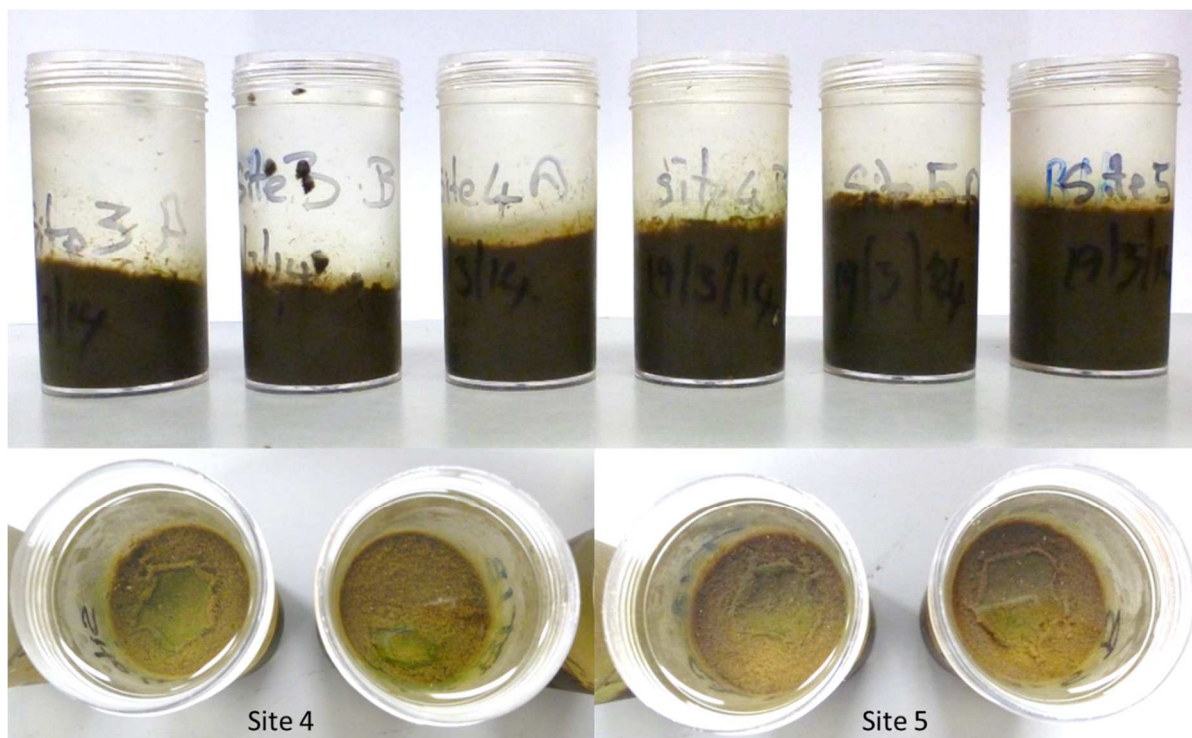


Figure C1: (Upper) Paired sediment trap sampling cups from sites 3, 4 and 5 from the 19 March 2014 study, (lower) top view into cups from site 4 and site 5 showing the mat that formed on the sediment surface. Just moving the trap cups caused the mat to curl up around the edges.